Lagrangian analysis of moisture sources of Tianshan Mountain precipitation

Xuefeng Guan, Lukas Langhamer, Christoph Schneider

Geography Department, Humboldt-Universität zu Berlin, Berlin, Germany

Key Points:

- A Lagrangian moisture source detection technique is applied to reveal the moisture sources of precipitation in the Tianshan Mountains.
- Local evaporation and Central Asia play a leading role in providing moisture for all sub-regions of the Tianshan Mountains.
- The moisture from East and South Asia (ESA) and Siberia during extreme precipitation months is significantly enhanced in the Eastern Tianshan.

Corresponding author: Xuefeng Guan, xuefengg@geo.hu-berlin.de

Abstract

The moisture sources of precipitation in the Tianshan Mountains, one of the regions with the highest precipitation in Central Asia during 1979-2017 are comprehensively and quantitatively summarized by using a Lagrangian moisture source detection technique. Continental sources provide about 93.2% of the moisture for precipitation in the Tianshan Mountain, while moisture directly from the ocean is very limited, averaging only 6.8%. Central Asia plays a dominant role in providing moisture for all sub-regions of the Tianshan Mountains. For the Western Tianshan, moisture from April to October comes mainly from Central Asia (41.4%), while moisture from November to March is derived primarily from Western Asia (45.7%). Nearly 13.0% of moisture to precipitation for Eastern Tianshan in summer originates from East and South Asia, and the Siberia region. There is a significant decreasing trend in the moisture contribution of local evaporation and Central Asia in the Eastern Tianshan during winter. The contribution of moisture from Europe to summer precipitation in the Central and Eastern Tianshan and the contribution of the North Atlantic Ocean to summer precipitation in the Northern, Central, and Eastern Tianshan also exhibit a decreasing trend. The largest increase in moisture in Western Tianshan stems from West Asia during extreme winter precipitation months. Europe is also an important contributor to extreme precipitation in the Northern Tianshan. The moisture from East and South Asia and Siberia during extreme precipitation months in both winter and summer is significantly enhanced in the Eastern Tianshan.

1 Introduction

The Tianshan mountains form a prominent so-called water tower in Central Asia providing major parts of the water resources of the surrounding lowlands (Immerzeel & Bierkens, 2012; Y. Chen et al., 2016). These water resources are essential for ecosystems, agriculture, and water supply for millions of people in Central Asia (Ososkova et al., 2000). Water resources stem from direct precipitation and runoff, seasonal snowmelt as well as meltwater from glaciers and permafrost (Armstrong et al., 2019; Sorg et al., 2012). The glaciers of the Tianshan mountains host the largest amount of fresh water in Central Asia and have a crucial function on the water cycle in the generally arid region of Central Asia (Aizen et al., 1997). Therefore, meltwater from Tianshan is a vital resource for the more than 100 million people living in the arid and semi-arid regions of Central Asia (Lemenkova, 2013; Bekturganov et al., 2016; Xenarios et al., 2019). However, driven by global warming Cen-

tral Asia has warmed significantly in recent decades, with a rate of 0.36–0.42°C/10a during 1979–2011 (Z. Hu et al., 2014), resulting in a pronounced glacier retreat and decrease in snow accumulation in Tianshan Mountains (Aizen et al., 2006; Farinotti et al., 2015). About 97.52% of the glaciers in the Tianshan Mountains show retreating trends from the 1960s to 2010s (Y. Chen et al., 2016) which is in accordance with the increasing temperature trend over decades (R. Hu, 2004; Yuan-An et al., 2013). On the contrary, precipitation in the Tianshan has shown an overall upward trend (Sorg et al., 2012; S. Wang et al., 2013; Y. Chen et al., 2016; Guan et al., 2021b; Yang & He, 2003; H. Zhang et al., 2009; Yuan et al., 2004; Fan et al., 2022), although some studies suggest that a significant decrease in precipitation has been observed in Western Tianshan (Guan et al., 2021b; Z. Hu et al., 2017). In addition to interannual variability, there is also multi-scale decadal variability in Tianshan precipitation (Guan et al., 2021b). By using the ensemble empirical mode decomposition (EEMD) method, Guan et al. (2021a) found that Tianshan winter precipitation has a multi-decadal oscillation of 26.8 and 44.7 years, and a positive anomaly after 1988. While summer precipitation has a significant 33.5 years multi-decadal pattern combined with a nonlinear increasing trend. Both, large-scale atmospheric circulation and individual weather patterns are key components controlling precipitation and its temporal variability in the Tianshan Mountains.

The Eulerian approach is a common method in studies of regional water vapor transport (Gimeno et al., 2012; Xingang et al., 2007). Previous diagnostics using the Eulerian method have revealed that the mid-latitude westerlies control the water vapour transport towards Tianshan. The location and intensity of the westerly jet varies seasonally and is subject to predominant synoptic patterns (Schiemann et al., 2008; Bothe et al., 2012; Yatagai et al., 2012; Yang & He, 2003). It influences the advection of moisture towards the Tianshan mountains and thus controls the moisture transport from the Atlantic Ocean, the Mediterranean, and the high latitudes (Aizen et al., 1997; Xingang et al., 2007; Huang et al., 2013). For instance, the westerly jet axis expands southward in winter and water vapor is advected mainly from the southwest towards Tianshan (Bothe et al., 2012). Additionally, there is moisture entering the southwestern Tianshan from Iran and Afghanistan, which is associated with the intrusion of warm and moist tropical air masses (Aizen et al., 1997). Contrary, during summer the westerly wind belt moves northward and there is an increase in water vapour flux from the north and northwest towards the Tianshan Mountains (Bothe et al., 2012; Huang et al., 2015; Guan et al., 2019). Guo et al. (2014) traced the long-range

oceanic water vapour sources affecting the Tianshan region, suggesting that the moisture sources in the Tianshan during the summer mainly originate from the sub-tropical North Atlantic Ocean, the Bay of Bengal, the Arabian Sea, and the northern Arctic Ocean. The Asian monsoon also influences the water vapour transported to the Tianshan Mountains. During warm El Niño–Southern Oscillation (ENSO) events, anomalous southwestern water-vapor fluxes from the Arabian Sea and tropical Africa enter Western Tianshan (Mariotti, 2007). In addition to the Eulerian perspective, the isotopic signature of stable water isotopes is often used to analyse the leading atmospheric mode of variability and changes. Results from such studies confirm that precipitation is controlled by the location of the westerly wind belt and the Indian monsoon (Feng et al., 2013). Simultaneously, the East Asian monsoon may influence precipitation in the westerly and monsoon transition zones (J. Yao et al., 2021). S. Wang et al. (2017), however, pointed out that moisture in the Tianshan Mountains is more likely to be locally sourced. (Song et al., 2019) stated that the moisture in Urumqi Glacier No.1 mainly comes from Europe and Central Asia, while the local contribution ranges from 46.8% to 52.1%. It should be mentioned that the Eulerian approach is able to show moisture pathways and moisture transport intensity, but fails to present a quantitative contribution of individual moisture sources to precipitation (Gimeno et al., 2012). Besides, the stable water isotope measurements and analyses also have their limitations and ambiguities due to the complex sensitivity of isotope signals to various drivers, and issues related to the mixing of isotopic signatures from various sources into few overall quantities. (Gimeno et al., 2012).

The Lagrangian methods have gained popularity in diagnosing moisture transport, especially in determining the origin of moisture deposited in specific areas (Stohl & James, 2004; Gimeno et al., 2010; Nieto et al., 2006; Durán-Quesada et al., 2010). The main advantage of the Lagrangian approach is the ability to provide more precise details about the moisture variation of the air parcels during transport (Gimeno et al., 2012). It allows simulating the backward trajectory of the air parcel in order to quantitatively describe the transport process and to identify the source of moisture (Stohl & James, 2004; Sodemann et al., 2008). Additionally, the Lagrangian analysis is particularly suitable for climatological studies over decades due to its lower computational cost compared to the more complex Eulerian moisture tagging approach (Winschall et al., 2014). Numerous attempts have been performed to determine the moisture sources by using Lagrangian methods (Knippertz & Wernli, 2010; Ramos et al., 2016; Sun & Wang, 2014; Langhamer et al., 2021). Concerning

moisture sources of precipitation in Xinjiang Province of China, S. Yao et al. (2021) used the Lagrangian diagnostic model FLEXPART to examine the moisture sources contribution to summer precipitation, concluding that local and Central Asian contributions amount to over 80%. Similarly, Hua et al. (2017) identified the moisture contribution by using a dynamical recycling model (DRM) modified by the Lagrangian method, suggesting that the moisture contribution of summer precipitation in northern Xinjiang during 1982-2010 was limited from the ocean. The major part of the moisture seems to be derived from land evaporation in Central Asia, western Siberia, eastern Europe, and northeastern Europe. Huang et al. (2017) tracked the backward trajectories of extreme precipitation in northern Xinjiang by the Lagrangian trajectory model HYSPLIT. They state that additionally to trajectories for rainstorms of above 100 mm d^{-1} originating from the North Atlantic, the Arctic Ocean, and Eurasia, there is also an anomalous branch from the Indian Ocean, which is closely associated with stronger meridional circulation and especially important for intense precipitation (Huang et al., 2017). W. Wang et al. (2020), also used the HYSPLIT model but traced the air particles rather than the actual moisture. They point out that in winter, western Eurasia contributes the most moisture to the precipitation in northern Xinjiang, reaching 48.11%. According to these authors, the amount of water vapor contributed by western Eurasia and the Arctic Ocean to northern Xinjiang shows an increasing trend from 1981-2017 (W. Wang et al., 2020).

Although there are many studies using the Lagrangian approach for some Central Asian sub-regions, especially the Xinjiang province in China, detailed quantitative calculations and temporal analysis of moisture fluxes to the Tianshan Mountains themselves are still missing. Besides, some studies taking the Lagrangian perspective have either not considered tracking actual moisture (Huang et al., 2017) or have not taken into account changes in specific humidity along the route (W. Wang et al., 2020). Further, seasonal precipitation varies greatly in the Tianshan sub-regions: precipitation in the Western Tianshan is concentrated in spring and winter while the Northern Tianshan receives the most precipitation in spring and the least in winter. Both the Central and Eastern Tianshan receive the highest precipitation in summer (Aizen et al., 1997; Guan et al., 2021b). Accordingly, we hypothesize that the Tianshan sub-regions are served by somewhat different moisture sources in different seasons, in addition to moisture from the west or Central Asia with the highest flux along the mid-latitude westerly wind belt.

Based on the lack of research in this respect and the advantages of the Lagrangian approach, we analyse the main moisture sources of the Tianshan Mountains. The temporal variability and quantitative contribution of moisture sources and favored moisture transport trajectories are investigated in detail using a verified Lagrangian moisture detection technique (Sodemann et al., 2008). We focus on four Tianshan sub-regions divisions, namely (1) Western Tianshan, west of Lake Issyk-Kul, (2) Northern Tianshan, north of Lake Issyk-Kul, (3) Central Tianshan, south of Ili Valley, (4) Eastern Tianshan, east of the cities of Urumqi and Dabancheng in China, following the approach taken in (Guan et al., 2021b, 2021a). For a more detailed description see section 2.1. We then use the Lagrangian analysis tool to present (a) spatial and temporal moisture flux patterns to the Tianshan Mountains, and (b) the differences in the main moisture sources between seasons in the four Tianshan Mountains sub-regions. Therefore, the manuscript is arranged as follows: The study area, the model, and all methods are introduced in Section 2. The model assessment is documented in Section 3.1. The moisture source patterns and quantitative contributions from individual moisture source regions to precipitation are presented in Section 3.2 and Section 3.3. Discussion and conclusion are presented in Sections 4 and 5.

2 Study area, data and methods

2.1 Study area

Tianshan Mountains, are a large mountain system in Central Asia, extending 2500 km from 66°E to 95°E, with an average width of 400 km which mainly straddles the border between China and Kyrgyzstan (Figure 1). The average elevation of the Tianshan Mountains is about 5 km, with the highest peak being Tomur Peak at 7,439 meters (42.03 °N, 80.13 °E). Bounded by Issyk-Kul Lake, the eastern edge of Kirgizskiy Alatau and the Fergana range (boundary 1), the area west of Issyk-Kul Lake is Western Tianshan. The prevailing air masses are carried into the Tianshan Mountains by moisture-filled westerly winds, and most of the precipitation falls on the windward western slopes, which results in the overall heaviest precipitation in the Western Tianshan. The Western Tianshan is under the combined influence of the southwestern branch of the Siberian anticyclone (although to a lesser extent) and southwestern cyclonic activity during the cold season, resulting in precipitation occurring mainly in winter and spring. In summer, the influence of subtropical high pressure leads to the least precipitation in the Western Tianshan during that season. Northern Tianshan lies to the north of Issyk-Kul Lake. In contrast to the Western Tianshan, which

receives the most precipitation in winter, the Northern Tianshan is strongly influenced by the Siberian anticyclonic circulation, resulting in the least amount of winter precipitation. The most precipitation occurs in spring, related to the development of frontal cyclonic circulation and the influx of cold and wet air masses. Central Tianshan is located in the south of Ili Valley and is bounded by the Fergana range to the west and by the Kokshaal Too and Meridionalniy ranges to the south and east. Being surrounded by high mountains prevents the entry of moisture, resulting in very little winter precipitation in the Central Tianshan, which only accounts for less than 10 % of the annual precipitation (Aizen et al., 1995; Guan et al., 2021b). Convection development and unstable atmospheric stratification together with humid and cold air from the west bring about the maximum precipitation during summer. Border 3 is bounded by the city of Urumqi and Dabancheng in China. To the east, the Eastern Tianshan (Region IV) includes the Bogda and Balkan mountain ranges. The seasonal distribution of Eastern Tianshan precipitation is the same as in Central Tianshan, with the most precipitation occurring in summer. However, as the area is the least affected by the East Asian monsoon and westerly circulation, the Eastern Tianshan receives much less precipitation than the rest of the Tianshan Mountains, averaging only 13 mm in winter (Guan et al., 2021b).

2.2 Data

The basis of the study comprises reanalysis data from the numerical weather prediction model ERA-Interim provided by the European Centre for Medium-Range Weather Forecasts (ECMWF) (Berrisford et al., 2011; Dee et al., 2011; Owens & Hewson, 2018) from 1979 to 2017. The usage of reanalysis data is beneficial specifically in remote mountainous regions with scarce observations (Gerlitz et al., 2014; Zhao et al., 2020). The reliability of ERA-Interim in Central Asia has been verified by long-term trend analysis (Z. Hu et al., 2016; Hamm et al., 2020; Liu & Zhang, 2017; S. Chen et al., 2019). We use the global ERA-Interim reanalysis dataset with its horizontal resolution of $0.75^\circ \times 0.75^\circ$ and 60 vertical levels, from the surface to 0.1 h Pa. In particular, the 3-D wind field, the specific humidity, the surface pressure, the Planetary Boundary Layer (PBL) height, and the 2-m air temperature serve as input variables to perform a moisture source detection study. The PBL height is scaled by the factor of 1.5 to counteract the underestimation of the PBL height specifically over maritime and mountainous terrain (Sodemann et al., 2008; Weigel et al., 2007; Zeng et al., 2004). The conversion into pressure coordinates considers a constant lapse rate of

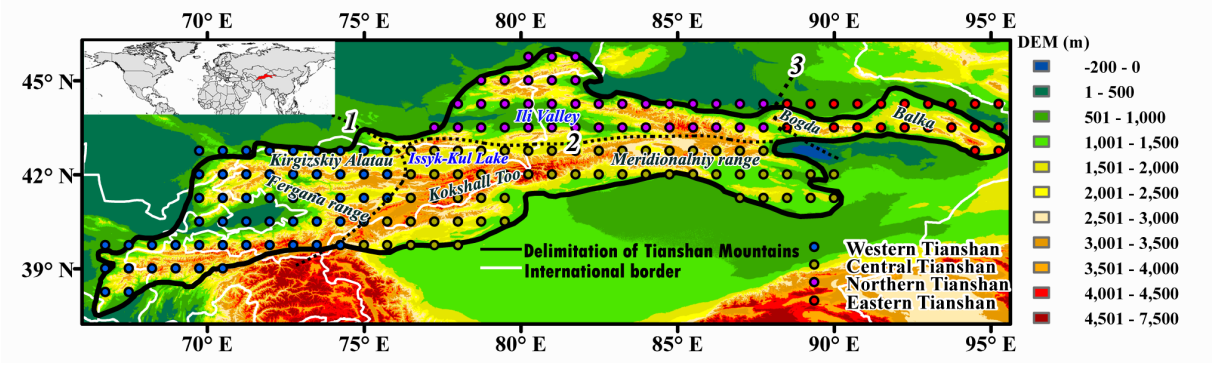

Figure 1. Topography of the study area and the starting points of backward trajectories within the Tianshan mountains. The dotted lines numbered 1 to 3 refer to the borders between the four sub-regions of the Tianshan Mountains detailed in the text. The red area in the small map in the upper left corner shows the position of the Tianshan Mountains in the Northern Hemisphere. Four differently colored sets of dots represent the initial positions over the Western Tianshan (blue dots), Northern Tianshan (purple dots), Central Tianshan (yellow dots), and Eastern Tianshan (red dots).

$\gamma = 0.0065\,\mathrm{K\,m^{-1}}$ (Langhamer et al., 2018). Additionally, we use the ERA-Interim monthly precipitation data, and the precipitation product from the Global Precipitation Climatology Centre (GPCC) (Schneider et al., 2018) to validate the performance of the Lagrangian model.

2.3 Lagrangian method for determining evaporative moisture sources

The Lagrangian perspective transforms the spatially stationary point of view from gridded reanalysis data into that of traveling air parcels. Along trajectories, changes in physical quantities such as moisture, air pressure, and temperature can be analyzed. We apply the Lagrangian analysis tool Version 2.0 (LAGRANTO) (Sprenger & Wernli, 2015), version 1.0 by (Wernli & Davies, 1997) to calculate trajectories 15 days backward in time. The backward trajectories start from a 0.75° regular grid within four predefined sub-regions encompassing the Tianshan Mountains. The grid is vertically subdivided in 11 equally spaced ($\Delta p = 50\,\mathrm{h\,Pa}$) levels from the surface to 500 h Pa above ground level which encloses the majority of the precipitable water of the Tianshan Mountains. This set-up comprises 242, 407, 594, and 616 grid points in Eastern, Northern, Western and Central Tianshan (Figure 1). Every reanalysis time step of 6 hours contains 242, 407, 594, and 616 15-d

backward trajectories, respectively. This results in over 200 million trajectories to represent a 37-year climatology of moisture sources of the Tianshan Mountains. Thereby the moisture source detection method developed by Sodemann et al. (2008) was applied, which is based on the moisture tracing the concept of Stohl and James (2004). This method includes the conversation of specific humidity q within the air parcel of mass m where the increase in specific humidity within a calculation time step i of the trajectory results only from moisture uptake through evaporation E, while the decrease occurs due to precipitation P,

$$m\frac{dq_i}{dt} = E_i - P_i \quad . \tag{1}$$

Multiple moisture uptakes can occur along a 15-day backward trajectory. Therefore, all new moisture uptakes dq_j are weighted with respect to the amount of pre-existing moisture q_i resulting in a fractional contribution f_j of each moisture uptake location,

$$f_j = \frac{dq_j}{q_i} \quad . \tag{2}$$

Precipitation along the trajectory reduces the impact of the previously estimated moisture uptake and is partially subtracted according to their fractional contribution (Sodemann et al., 2008). The conversion of the specific humidity decrease $\Delta q_{k,t=0}$ above the study region into the 6 hourly precipitation sum can be expressed as,

$$P = -\frac{1}{g}\sum_k \Delta q_{k,t=0h} \cdot 10^{-3} \cdot \Delta p_k, \tag{3}$$

where g is the the gravitational acceleration, k is the vertical index of the 11 equidistant ($\Delta p_k = 4990\,\mathrm{h\,Pa}$) levels and is hereinafter called Lagrangian precipitation (Sodemann et al., 2008). Based on the Lagrangian precipitation and the fractional contribution of each moisture uptake along the trajectory, the amount of evaporation is calculated and assigned to the surface according to,

$$E_j = P_{i=0\,\mathrm{h}} \cdot f_m \quad . \tag{4}$$

Following the concept of Sodemann et al. (2008), only trajectories that cause precipitation are selected in the calculation. The selection criterion for trajectories was that the relative humidity exceeded 80% and the specific humidity decreases. Originally, Sodemann et al. (2008) considered only a moisture increase within the PBL as evaporative moisture source. Subsequently, Sodemann and Zubler (2010) deviate moisture sources within and above PBL moisture uptake. The authors concluded to consider moisture increase in the free atmosphere as evaporative moisture source only if the spatial and temporal pattern of

the combined above and below PBL moisture uptake shows similarities to the within PBL moisture uptake.

In addition, this study investigates linear trends of defined moisture sources in winter and summer using the Mann-Kendall (M-K) test (Mann, 1945; Kendall, 1975). We also use Mann-Kendall (M-K) correlation coefficient (Freedman et al., 2007) to assess the statistical significance of any correlation analysis.

3 Results

3.1 Characteristics of ERA-Interim precipitation, GPCC precipitation and Lagrangian precipitation estimates

At first, we validate the Lagrangian precipitation estimates (Equation 3) over the Tianshan Mountains against the 6-hourly forecasts from ERA-Interim and the GPCC precipitation. The spatial distributions of ERA-Interim precipitation over Tianshan Mountains are shown in Figures 2(e)-2(h). Precipitation over the Tianshan Mountains has a strong seasonality with the larger precipitation amounts in MAM and JJA. Regionally, the western part of Tianshan receives the most precipitation and Eastern Tianshan has relatively less precipitation throughout the year. These spatial and seasonal distributions are further confirmed by the GPCC precipitation (Figures 2(i)-2(l)). However, the precipitation from ERA-Interim is obviously higher than that from the GPCC. Previous studies have found that mountainous and complex topographic areas result in large differences in precipitation between products (Hamm et al., 2020). Gao et al. (2018) reported ERA-Interim overestimation of daily mean and extreme precipitation on the Tibetan Plateau. Similar conclusions were drawn by Hamm et al. (2020), founding that total spatially averaged precipitation for the period May to September 2017 from ERA-Interim (781 mm) over the Central Himalaya and the Southwest Tibetan Plateau, was much higher than that from GPCC precipitation (411 mm).

Figures 2(a)-2(d) display the composite mean horizontal distribution of estimated precipitation based on the Lagrangian approach (Equation 3) over the Tianshan Mountains. The Lagrangian estimated precipitation reasonably captured the major spatial patterns and seasonality of precipitation in the Tianshan Mountains similar to ERA-Interim (Figures 2(e)-2(h)). The Lagrangian precipitation estimates are somewhat higher than the ERA-interim

precipitation when considering individual grid points. This is especially observed in the Western and Northern Tianshan.

Figure 3(a) visualizes the comparison of monthly precipitation between the three precipitation data sets. The Lagrangian precipitation and ERA-Interim precipitation as well as the Lagrangian precipitation and GPCC precipitation both show statistically significant correlations ($p \leq 0.05$) with R^2=0.98 and R^2=0.95, respectively. Nevertheless, the ERA-Interim precipitation does not fully reflect some of the details of the GPCC data. The peak of monthly precipitation occurs in May (Lagrangian precipitation and GPCC precipitation), while ERA-Interim displays a single peak with the highest value in June. Similarly, precipitation in October is higher than in September, a feature that is not picked up in the ERA-Interim data. In addition, Figure 3(b) demonstrates that the Lagrangian approach is quite efficient in the Tianshan Mountains. A statistically significant linear relationship ($\mathbf{R^2}$ = 0.99) is shown between monthly evaporation (the sum of evaporation above and within the boundary layer) and Lagrangian precipitation estimates. Therefore, following e.g. Langhamer et al. (2021); Schuster et al. (2021), it is plausible that we apply the Lagrangian method to detect moisture sources of the Tianshan Mountains.

3.2 Patterns of moisture sources of Tianshan precipitation

Figure 4(a), (b), and (c) show the diagnostic picture of all attributed moisture sources, the attributed evaporation inside the PBL and from above the PBL, respectively. Moisture sources within the PBL show a similar spatial pattern to that of all attributed moisture sources, with the highest evaporative moisture contribution area mainly concentrated in the Tianshan itself. Regions with moisture source contributions exceeding 0.2 mm/month concentrate in Western Tianshan. Moisture source contributions exceed 0.1 mm/month over the majority of Tianshan, indicating that local evapotranspiration (i.e., recycling of continental moisture) are the major moisture source in the Tianshan Mountain. In addition, much of the moisture was also tracked back to West Asia, and even the Arabian Gulf. It is worth noting that the location of the annual mean source of moisture uptake above the PBL (Figure 4c) is quite similar to the location within the PBL (Figure 4b). Although, according to the Lagrangian approach, the location of the moisture source can only be determined when an increase in specific humidity below the top of the PBL is measured (Sodemann et al., 2008). However, Sodemann and Zubler (2010) pointed out that if the patterns of moisture sources above and within the PBL are similar, it is hardly possible

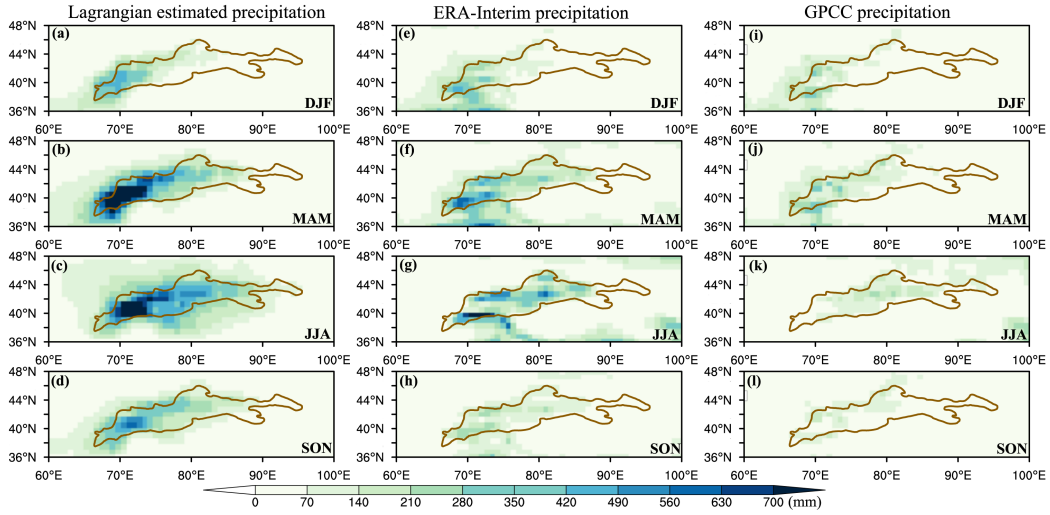

Figure 2. Spatial distribution of seasonal precipitation in Tianshan Mountains (mm) from the ERA-Interim Lagrangian estimated precipitation (left), the ERA-Interim monthly precipitation (middle), and the GPCC precipitation (right) during 1979 - 2017. All datasets are averaged in the four seasons: March-May (MAM), June-August (JJA), September-November (SON), and December-February (DJF). The area of the Tianshan Mountains is delineated with an earthly yellow polygon.

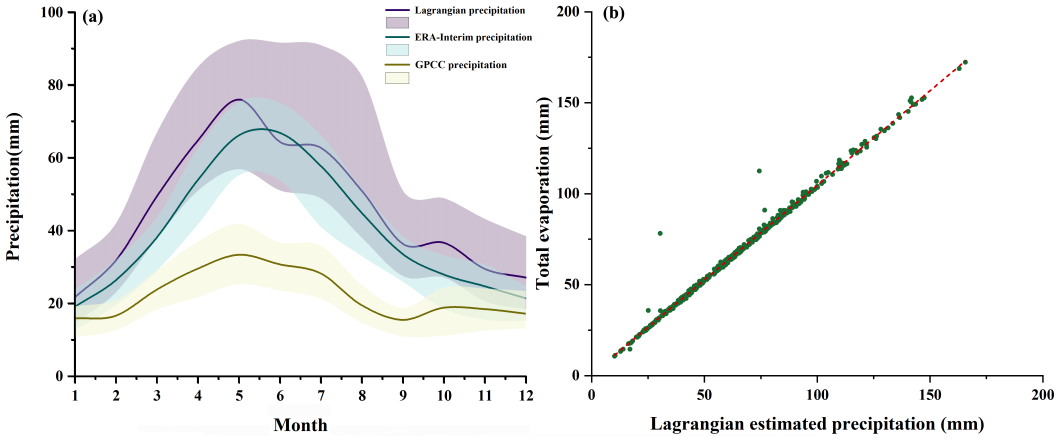

Figure 3. (a) ERA-Interim estimated monthly precipitation in the Tianshan Mountains, compared with that derived from the ERA-Interim and GPCC precipitation. The solid lines are the median; the areas filled correspond to the interquartile range. (b) The monthly Lagrangian estimated precipitation and the total local evaporation of the Tianshan Mountains.

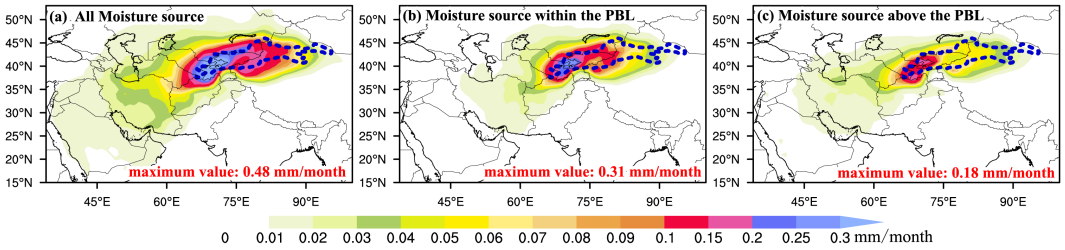

Figure 4. Spatial patterns of (a) all average annual attributed evaporative moisture sources (mm/month); (b) average annual attributed evaporative moisture sources within PBL; (c) average annual attributed evaporative moisture sources above the PBL of the Tianshan precipitation for the period from 1979 to 2017. The curve in blue dashed is the border of the Tianshan Mountains.

that the moisture sources of precipitation in the study area can be significantly different within and above the PBL. Therefore, in the following, we attribute the increase in specific humidity above the PBL also to evaporation from the surface, i.e., consider all the attributed moisture as the sources of precipitation in the Tianshan Mountains.

We subdivide the moisture sources presented into two seasons, thereby, October-March denoted as winter, and April-September as summer. South-westerly water vapour flux prevails into the Tianshan Mountains in winter (Figure 5e). Low latitudes and the Atlantic Ocean regions show relatively high precipitable water vapour (PWC) values compared to low PWC values over Central and East Asia including the Tianshan Mountains themselves. From the Euler perspective, there are two main water vapour pathways into the Tianshan Mountains in winter. One of them is a long-range water vapor transport pathway, advected predominantly by westerlies, extending from the Atlantic Ocean, the European continent, the Mediterranean Sea, and the Caspian Sea to the Tianshan. The second most important moisture pathway towards Western Tianshan stems from the Indian Ocean and the Arabian Peninsula (Figure 5e). From the Lagrangian perspective (Figure 5a-d), the moisture sources of Tianshan extend as far west as 30°W over the Atlantic Ocean based on a minimal lower threshold of 0.0002 mm/month. Areas with larger moisture uptake are mainly located over Central and West Asia, with the highest values centered in and around the Western Tianshan. Although the moisture-source regions in winter of the different sub-regions of Tianshan Mountains look relatively similar, the source area for the Western Tianshan is markedly expanded both to the west and to the southeast (Figure 5a). In contrast, uptake locations for the Central Tianshan are confined to areas east of the Prime meridian (Figure

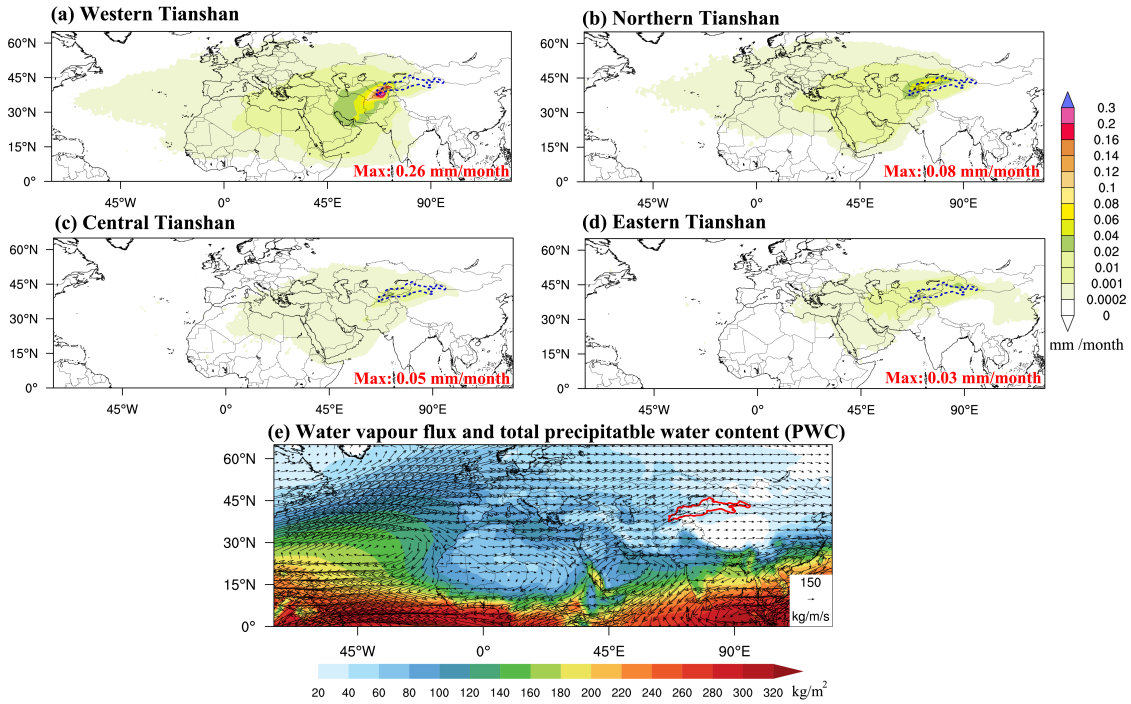

Figure 5. Spatial patterns of average attributed evaporative moisture sources (mm/month) of the different sub-regions (a)-(d) of the Tianshan mountains in winter; the polygon in blue dashed is the border of the Tianshan Mountains; (e) Water vapour flux (vector in kg/m/s) and total precipitable water vapour content (PWC in kg/m^2) in winter. The area of the Tianshan Mountains is delineated with a red polygon in (e).

5c). The area of uptake for the Eastern Tianshan is even narrower to roughly east of 30°E (Figure 5d). Regions with evaporative moisture sources for the Western Tianshan exceeding 0.1 mm/month have a widespread distribution that extends southwestward to the Iranian Plateau. Areas outside the Tianshan with evaporative moisture sources exceeding 0.1 mm/month are rare for the other three Tianshan sub-regions. Moisture sources for the Western Tianshan in winter extend southeastward to the Indian Peninsula until 80°E using a threshold of 0.0002 mm/month, which is not the case for any of the other Tianshan sub-regions.

PWC values in summer are higher ($> 125\,kg/m^2$) over the continental regions at mid–to-high latitudes compared to winter (Figure 6e). The presence of the Iranian High Pressure advects water vapour from high-latitude Eurasia towards the Tianshan Mountains. Meanwhile, this anticyclone blocks water vapour entering the Tianshan from the southwest.

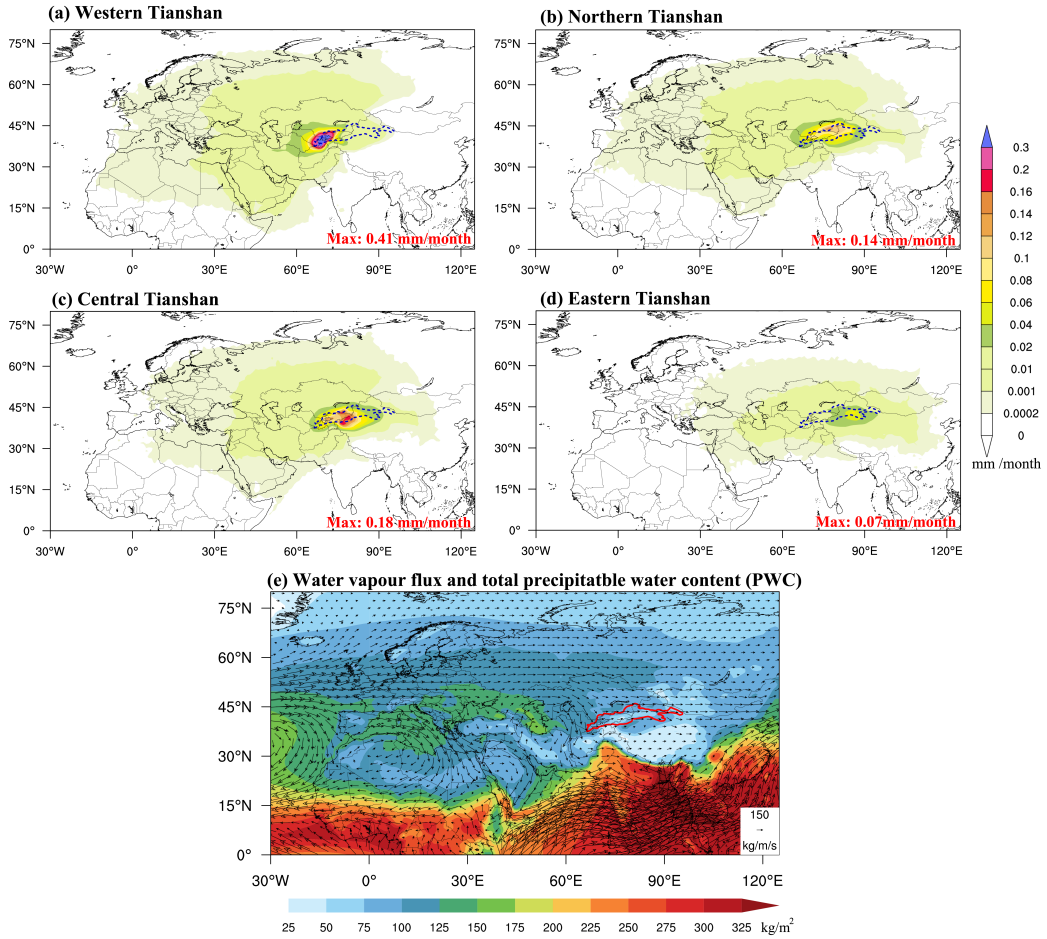

Figure 6. Spatial patterns of average attributed evaporative moisture sources (mm/month) of the four sub-regions (a)-(d) of the Tianshan Mountains in winter; the curve in blue dashed is the border of the Tianshan Mountains; (e) Water vapour flux (vector in kg/m/s) and total precipitable water vapour content (PWC in kg/m^2) in summer. The area of the Tianshan Mountains is delineated with a red polygon in (e).

In summer, the area of moisture contribution is generally smaller to the west and to the south, confined to areas east of the Prime meridian (Figure 6a-c). The moisture source of the Eastern Tianshan is limited to east of 30°E (Figure 6d). The moisture contribution is more locally concentrated. The area of moisture uptake in the high latitudes of Eurasia expands further to 75° N with an increased contribution from high latitude Eurasia. Simultaneously, the contribution from the Arabian Peninsula and the Iranian Plateau is smaller than in the winter. The summer moisture source in the Eastern Tianshan extends even further eastward to 120°E in East Asia (Figure 6d).

3.3 Quantitative contribution from individual moisture source regions

The previous section showed that sources of water vapor contributing to precipitation in the Tianshan Mountains extend in the West to the Atlantic Ocean and Europe, in the North to Europe, in the Southwest to West Asia and the Indian Ocean, and in the Northeast to East Asia and Siberia. To more precisely describe the key moisture sources of precipitation in Tianshan Mountains, we define 10 separate moisture uptake regions in the Northern Hemisphere (Figure 7) and additionally the Tianshan Mountains themselves (TS) as the source region of local evaporation following an approach similar to (Sodemann et al., 2008) and S. Yao et al. (2021). The terrestrial part includes Central Asia (CA) where the Tianshan Mountains are located, West Asia (WA) and North Africa (NA), and the European region (EU) which lies to the northwest of the Tianshan Mountains. We further separate into the Siberian region (SR) and East and Southeast Asia (ESA) in the east of the Tianshan Mountains. The oceanic part includes the North Atlantic Ocean (NO), the Mediterranean Sea (MS), the Caspian Sea (CS), and the Indian Ocean (IO). Some inland seas, such as the Baltic Sea and the Black Sea, are incorporated into the European region owing to their low contribution and their location within Europe. The contribution of a particular region is evaluated as the ratio of the integral of its moisture contributing area to the integral of all identified moisture contributing areas. The 11 areas shown in Figure 9 contribute more than 99.5% of all moisture flux to the precipitation in the Tianshan Mountains. Hence, all key moisture source areas of precipitation over the Tianshan Mountains are included in this assessment.

Central Asia is the dominant source of moisture for all sub-Tianshan. For the Western Tianshan, the contribution of Central Asia shows a single-peak pattern (Figure 8a). From April to October, Central Asia is the major contributor of moisture in the Western Tianshan, with a contribution of on average 41.4%, and 46.3% in August (Figure 8a). In contrast, from November to March, West Asia replaces Central Asia as the largest source of moisture in providing precipitation for the Western Tianshan, accounting for almost 50% of the total. The third source of moisture stems from the Tianshan itself (local evaporation) with 17.2%, also showing a single-peak pattern in summer. Moisture from the Indian Ocean also contributes considerably (7.2%) to precipitation in the Western Tianshan in winter, while Europe contributes 9.5% of the precipitation in summer (Figure 8a). For Northern Tianshan, the continent is the most vital moisture source for precipitation (Figure 8b). The four moisture source regions with mean relative contributions $\geq 5\%$ include local evaporation

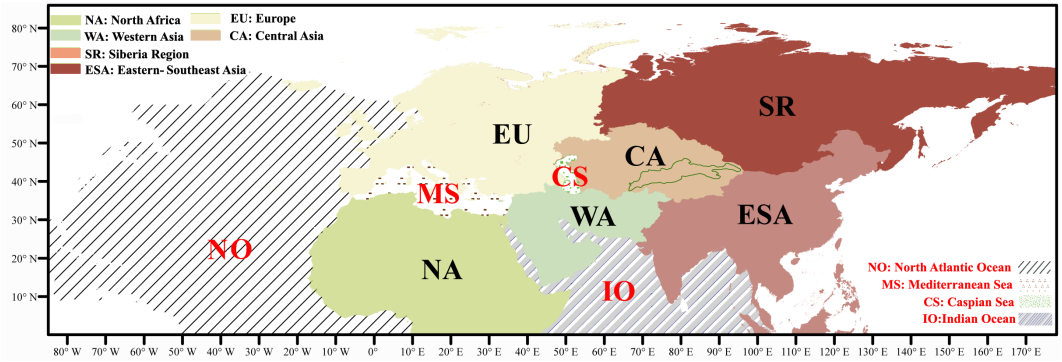

Figure 7. Definition of the ten regions for diagnosing and attributing moisture sources in this study: Central Asia (CA), West Asia (WA), North Africa (NA), Europe (EU), Siberia (SR), East and Southeast Asia (ESA), North Atlantic Ocean (NO), Mediterranean Sea (MS), Caspian Sea (CS), and Indian Ocean (IO). The area of the Tianshan Mountains (TS) defining the area of local evaporation is delineated with a green polygon.

(22.5%), Central Asia (37.0%), West Asia (19.5%), and Europe (7.3%). It is noteworthy that the local moisture contribution accounted for 46.6% in August, providing the largest source of moisture in the Northern Tianshan. The moisture contribution to the Central Tianshan is very similar to the monthly distribution of the Western Tianshan, although local evaporation provides a very uniform share throughout the year of about one-third. The relative contribution of moisture from Central Asia to the Central Tianshan is larger than to the Western Tianshan and also more evenly distributed across seasons (Figure 8c). In addition to the largest contribution coming from Central Asia and local evaporation (66.8%), West Asia adds another 18.0%. Hence, these three regions contribute up to almost 85% of the moisture to the Central Tianshan. For the Eastern Tianshan, Central Asia is the moisture source with an unassailable position of precipitation in all seasons, accounting for above 45% (Figure 8d). It is followed by local supply, evenly distributed in all months except for March, and overall accounting for 23.4%. The other two moisture sources with mean relative contributions of more than 5% are West Asia (10.4%) and Europe (5.3%), respectively. The contribution of Europe to summer precipitation in the Eastern Tianshan is reduced compared to that in winter. East and Southeast Asia, and the Siberian region, replacing Europe, are the other two important moisture sources with a percentage in summer of 7.7% and 5.2%, respectively (8d).

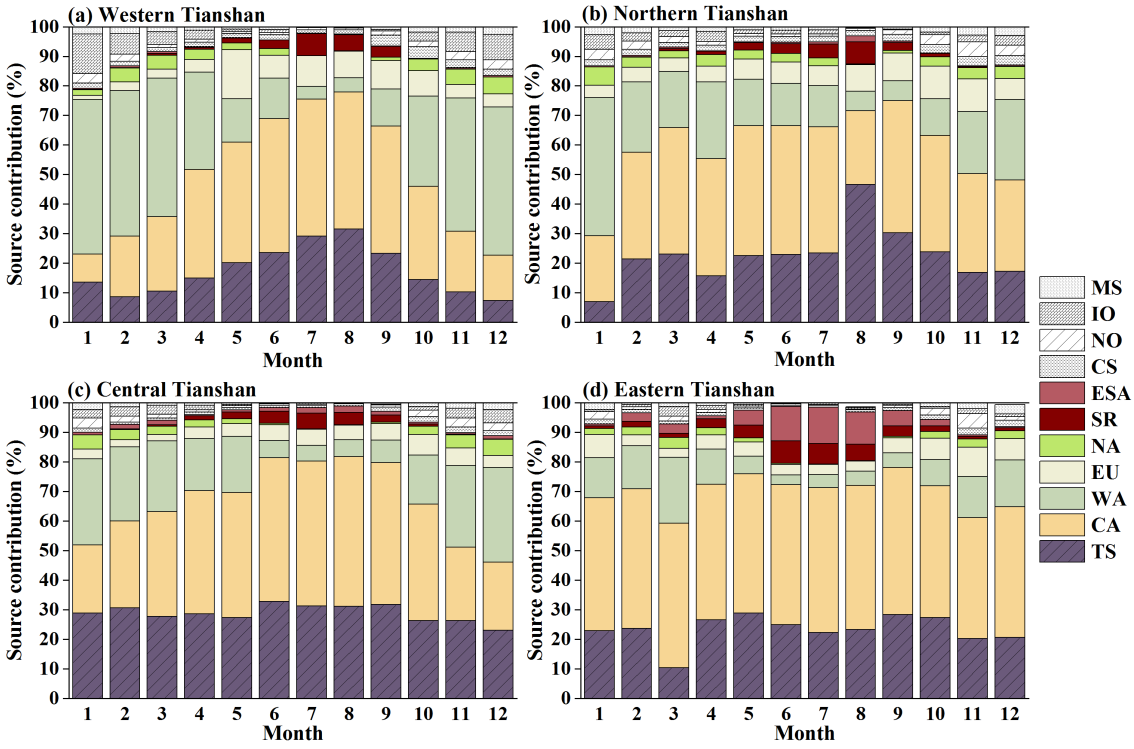

Figure 8. Monthly mean relative contribution of the different uptake sectors defined in Figure 7 to the attributable precipitation over the (a) Western Tianshan, (b) Northern Tianshan, (c) Central Tianshan, and (d) Eastern Tianshan.

We further investigate the possible correlations between the contribution of each identified moisture source area and precipitation in the Tianshan Mountains in winter and summer in the time series of annual values of the study period (Table 1). For the Western Tianshan, the winter precipitation sum is significantly positively correlated with the moisture contribution from West Asia and the Indian Ocean, and negatively correlated with the moisture contribution from local sources and Central Asia, strongly confirming that moisture from the southwest plays a dominant role in the increased winter precipitation in the Western Tianshan. Winter precipitation in the Western Tianshan is positively correlated with the moisture contribution from East and South Asia, implying that the source of moisture from the East to the Western Tianshan, although low, should not be neglected. Precipitation in the Northern Tianshan is significantly positively correlated with moisture contribution from the Caspian Sea and the Mediterranean Sea and negatively correlated with local moisture contribution in winter, reflecting the profound influence of the westerlies on winter precipitation in the Northern Tianshan. The winter precipitation in ERA-Interim shows no significant correlation with any moisture source in the Central and Eastern Tianshan, while precipitation in GPCC is positively correlated with moisture from North Africa and the Indian Ocean for the Central Tianshan and negatively correlated with local moisture contribution for the Eastern Tianshan (Table 1).

In general, there is no obvious trend in the contribution from most source regions in winter during 1979-2017. However, Tianshan, the region of local sources, and Central Asia show a significant decreasing trend ($p \leq 0.05$) of moisture contribution to the Eastern Tianshan in winter with linear trends of -0.30mm/10a and -0.11mm/10a, respectively (Figure 9). The finding is consistent with a decreasing trend in Winter precipitation in the Eastern Tianshan in the ERA-Interim data. However, (Guan et al., 2021a) derive a positive precipitation trend for the Eastern Tianshan in winter based on GPCC data for the same period.

Correlations between summer precipitation from ERA-Interim and GPCC in the Tianshan Mountains and the moisture source contribution vary widely. In general, summer precipitation in the Western Tianshan has a negative correlation with moisture from Europe and is positively correlated with moisture from East Asia. In addition, precipitation remains significantly positively correlated with moisture contribution from the southwest. Different from winter, the summer precipitation in the Northern Tianshan is negatively correlated with moisture flux from the Caspian Sea and the Atlantic Ocean (Table 1). Not

Table 1. Correlation between moisture uptake in the source areas according to Figure 7 and ERA-Interim precipitation based on seasonal values in the period 1979-2017; correlation coefficients with moisture uptake and GPCC precipitation are shown in parentheses. Mann-Kendall (M-K) correlation coefficients were calculated for winter and summer. Only coefficients of statistically significant correlations ($p \leq 0.05$) are presented in the table; WT: Western Tianshan, NT: Northern Tianshan, CT: Central Tianshan, ET: Eastern Tianshan.

	Winter				Summer			
	WT	NT	CT	ET	WT	NT	CT	ET
TS	(-0.26)	-0.27 (-0.33)		(-0.31)	(-0.41)		(-0.43)	
CA	-0.47 (-0.35)							
WA	0.29 (0.29)				(0.28)		(0.24)	
EU					-0.21		(-0.24)	
NA			(0.24)		(0.23)			
SR								0.41
ESA	0.32 (0.28)				0.23		(0.23)	
CS		0.23 (0.24)				-0.33		
NO						-0.22		
IO	0.30 (0.27)		(0.24)		0.24	(0.31)	(0.31)	
MS		0.34 (0.35)					(0.27)	

surprisingly, summer precipitation in the Eastern Tianshan is significantly positively correlated with moisture from Siberia. We find significantly decreasing trends of moisture contribution from the North Atlantic Ocean for Northern Tianshan (-0.05 mm/10a), Central Tianshan (-0.02 mm/10a) and Eastern Tianshan (-0.01 mm/10a) and from Europe for Central Tianshan (-0.06 mm/10a) and Eastern Tianshan (-0.03 mm/10a) over the study period (Figure 10). These trends do not play out in decreasing precipitation amounts according to (Guan et al., 2021a), presumably because their relative contribution to the overall precipitation in summer in the respective sub-regions of Tianshan is limited.

We selected monthly precipitation from ERA-Interim data exceeding the 95th percentile in winter and summer in each Tianshan region as extreme precipitation months. Clear differences in the spatial pattern of source regions of moisture received by the four sub-

Tianshan during extreme precipitation are evident in Figure 11 and Figure 12. Compared with the average evaporative moisture intake, the overall amount during extreme winter precipitation in Western Tianshan increased by 28.9%, with the main increase still coming from the southwest. (Figure 11(a)). The relative moisture contributions from West Asia and the Indian Ocean for extreme precipitation are 54.3% and 7.9% (Figure 13), with moisture uptakes increasing from 19.8 mm/month and 2.4 mm/month (average in winter) to 32.7 mm/month and 4.8 mm/month, respectively from these regions. The moisture contribution from Europe, on the contrary, decreases from 4.2% (winter average share) to 1.6%, a decrease of 69.2%, implying that extreme precipitation in the Western Tianshan in winter is caused by enhanced meridional moisture advection and weakened latitudinal moisture flux. For the Eastern Tianshan, the relative contributions from Siberia as well as from East and South Asia during winter extreme precipitation increase from 1.3% and 1.7% to 5.6% and 10.1%, respectively (Figure 13 (d)). The moisture uptakes increase from 0.03 mm/month and 0.01 mm/month to 0.50 mm/month and 0.94 mm/month, respectively (Figure 11 (d)), reaffirming the importance of moisture from the east for the Eastern Tianshan. Although Europe accounts for only 7.1% of the moisture contribution in the Northern Tianshan during winter (Figure 8), the largest increase of 64.8% in moisture contribution from Europe is observed during extreme winter precipitation, suggesting that moisture from Europe is an important cause of extreme precipitation in the Northern Tianshan, which is diametrically opposed to the Western Tianshan. For the Central Tianshan, Central Asian and local evaporation plays a crucial role during extreme precipitation, especially for Central Asia, where the relative contribution goes up from 29.1% (average in winter) to 39.3% (Figure 13). The increase in moisture uptake is close to 50% in both cases. However, it can be seen from the (Figure 11 (c)) that the regions of increased moisture contribution are concentrated in and around the Central Tianshan itself, demonstrating that the extreme winter precipitation moisture contribution in the Central Tianshan is derived from local evaporation. In contrast to winter, the increased moisture contribution during extreme summer precipitation is concentrated locally and in Central Asia, especially for the Central and Northern Tianshan (Figure 12. Not surprisingly, the contribution of moisture from Siberia as well as East and South Asia appears to increase during extreme precipitation in the Eastern Tianshan, with the relative moisture contributions from these regions increasing from 5.2% and 7.7% (summer average shares) to 9.9% and 18.5%, respectively (Figure 13).

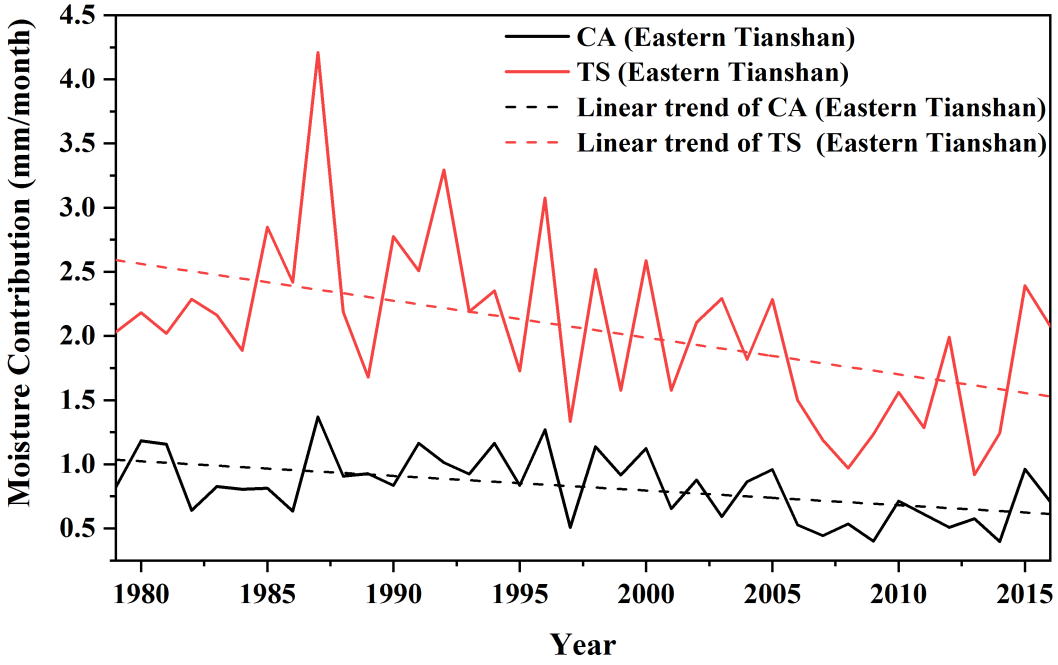

Figure 9. Time series of moisture contribution from Central Asia and local sources for the Eastern Tianshan in winter during the 1979-2017.

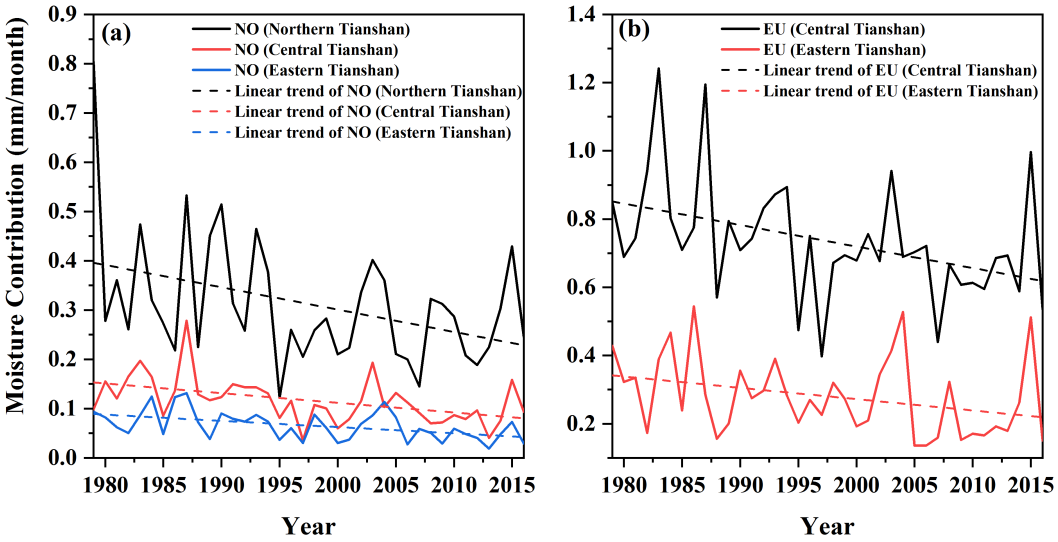

Figure 10. Time series of moisture contribution in summer from the North Atlantic Ocean for Northern, Central and Eastern Tianshan, respectively (a) and Europe (b) for Central Tianshan and Eastern Tianshan during 1979-2017.

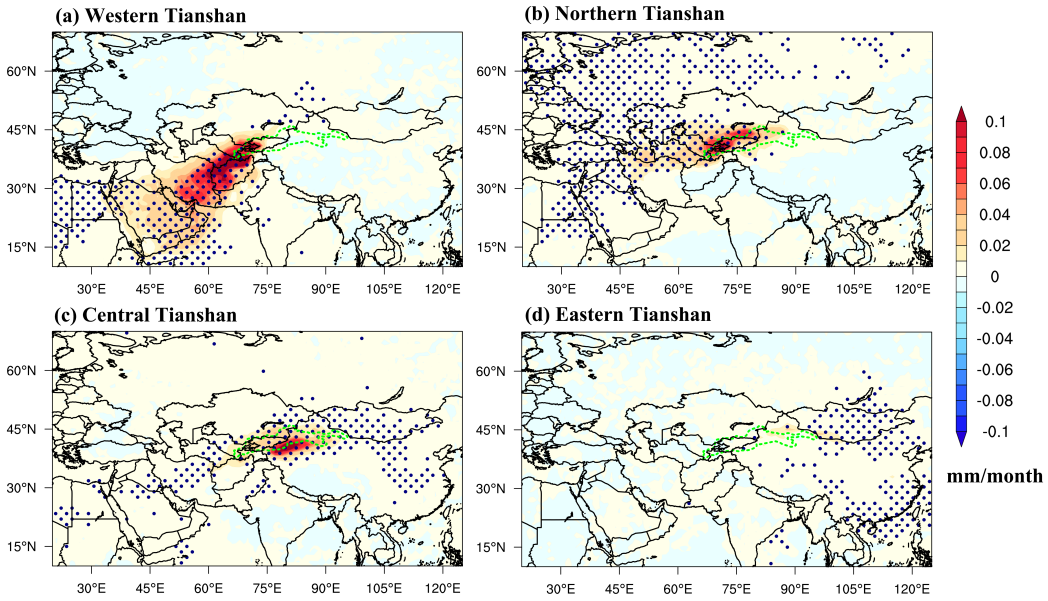

Figure 11. Anomalies of evaporative moisture sources during extreme winter precipitation in (a) Western Tianshan, (b) Northern Tianshan, (c) Central Tianshan, and (d) Eastern Tianshan. The area of the Tianshan Mountains is delineated with a green polygon and the blue dotted areas indicate anomalies that are significant at the 95% confidence level.

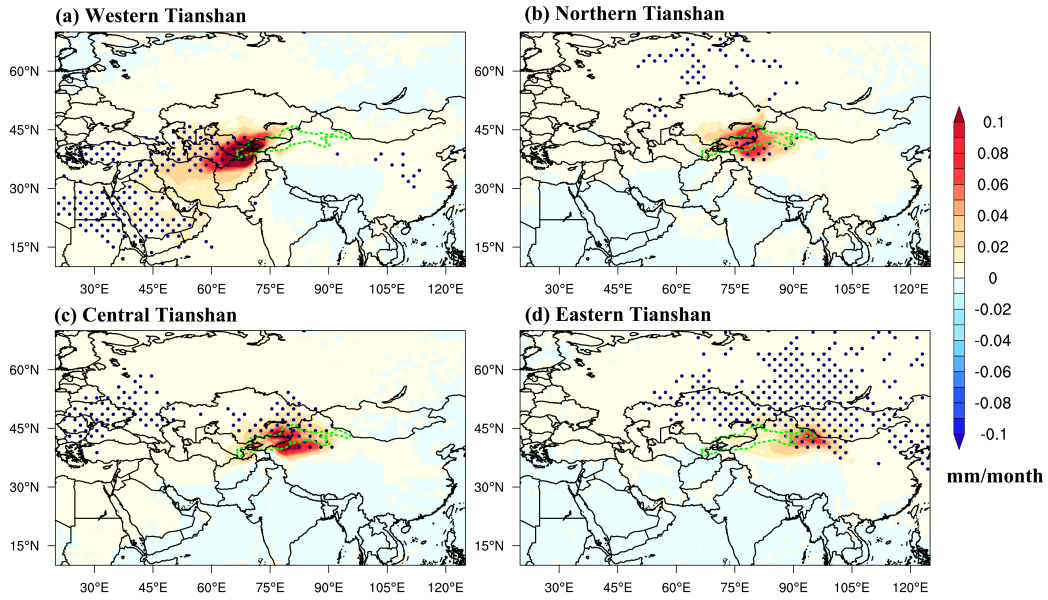

Figure 12. Anomalies of evaporative moisture sources during extreme summer precipitation in (a) Western Tianshan, (b) Northern Tianshan, (c) Central Tianshan, and (d) Eastern Tianshan. The area of the Tianshan Mountains is delineated with a green polygon and the blue dotted areas indicate where anomalies are significant at the 95% confidence level.

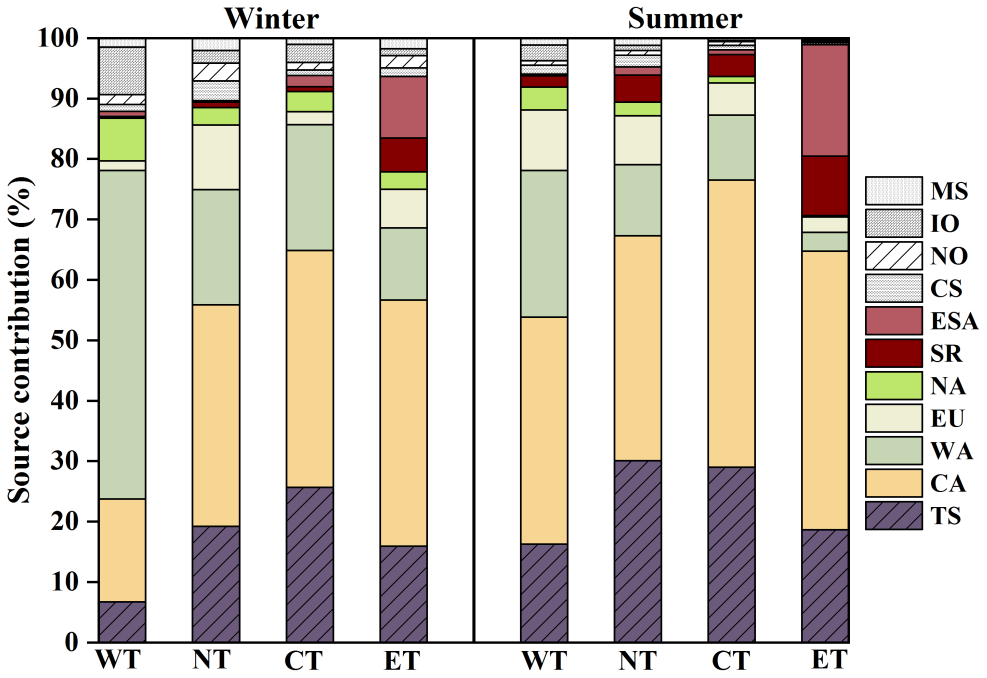

Figure 13. Monthly mean relative contribution of the different uptake sectors defined in Figure 7 to the attributable precipitation over the Western Tianshan (WT), Northern Tianshan (NT), Central Tianshan (CT), and Eastern Tianshan (ET) in winter and summer.

4 Discussion

According to Guan et al. (2021b), most parts of Tianshan experienced increasing precipitation during 1950-2016, especially in the Northern, Central, and Eastern Tianshan. They suggested possible reasons for the variability of precipitation in terms of atmospheric circulation. The East Atlantic-West Russia (EATL/WRUS) represents circulation variability affecting Tianshan precipitation in winter. The enhanced meridional features of the EATL/WRUS pattern after 1988 lead to enhanced water vapor entering the Tianshan from low latitude oceanic regions (Guan et al., 2021a). This is further corroborated by the results in this study presented in Figure 5 and Figure 8 that the dominating moisture sources of precipitation are mainly West Asia and Indian Ocean during winter for the Western Tianshan. Warm conveyor belts embedded ahead of the trough axis of extra-tropical cyclones transport water vapor from the lower latitudes poleward (Boutle et al., 2011). Hence, up to 70% of precipitation extremes can be associated with extra-tropical cyclones or warm conveyor belts that advect moisture from West Asia and the Indian Ocean towards Western Tianshan (Pfahl et al., 2014). However, it is worth noting that according to our results (Ta-

ble 1), the significantly positive correlation between winter precipitation and moisture from West Asia and the Indian Ocean exists only in the Western Tianshan and Central Tianshan, which implies that the EATL/WRUS pattern mainly affects the west of the Tianshan Mountains where precipitation is concentrated during winter. In addition, Oh et al. (2017) found that in winter, when EATL/WRUS have the same phase combined with the Western Pacific teleconnections (WP), strong southeasterly wind anomalies deliver warm air to be transported from the tropics to East Asia. As seen from Figure (14), positive northward anomalous moisture transport from the low-latitude sub-tropics to East Asia exists in the synthesis of extreme winter precipitation months for the Western and Central Tianshan. The water vapor can be conveyed to Mongolia as well as to Siberia, which is also reflected in the significant positive correlation between winter precipitation in Western Tianshan and evaporative moisture uptake from East and South Asia, and between winter precipitation in the Central Tianshan and evaporative moisture coming from Siberia (Table 1). In summer, the Scandinavia pattern (SCAND) is strongly and negatively correlated with precipitation in Western Tianshan (Guan et al., 2021b). A strong pressure gradient enhances airflow to the Tianshan Mountains due to a persistent anticyclone over the Ural Mountains combined with the Central Asian cyclone east of the Caspian Sea (Guan et al., 2021b; Yang & He, 2003). The strong easterly flow reduces the moisture carried from Europe during extreme summer precipitation months in the Western Tianshan (15 (a)), which is an expression of the negative correlation between the summer precipitation in the Western Tianshan and the moisture contribution from Europe (Table 1). East Asia-Pacific (EAP) is another important teleconnection pattern affecting Tianshan precipitation (Guan et al., 2021a). The enhanced flux of water vapour during 1985-2004 occurred westward from East Asia to the Tianshan Mountains related to the EAP pattern. Our findings also confirm the influence of East and South Asia on Tianshan precipitation, with an emphasis on the contribution to Eastern Tianshan. During extreme summer precipitation in Eastern Tianshan, there appears to be an anomalous meridional moisture flux attributable to an "anticyclonic-cyclonic-anticyclonic" structure in the West Pacific off the coast of East Asia and Siberia which is very similar to the EAP pattern (Figure 15 (b)). Further, water vapour is transported westward from East Asia through China and Mongolia by a cyclone centered over Japan, which makes East and South Asia contribute 18.5% of moisture during extreme summer months. The extreme rainstorm event in July 2018 in the southeastern region of Hami (located in the Eastern Tianshan region) was caused by the westward transport of water vapor even from

the remote South China Sea into the Hami region (Liu et al., 2020). Consistently, Fan et al. (2022) found that the North Pacific pattern (NP) and the Pacific interdecadal Oscillation (PDO) had an important impact on precipitation changes in Tianshan Mountains (the part within China) during 1979-2020, both of which indicate the influence of the Pacific Ocean on precipitation in the more eastern parts of the Tianshan Mountains. In addition, the anomalous anticyclone located in western Siberia conveys moisture from Siberia to the Eastern Tianshan, accounting for the increased moisture contribution from Siberia of 9.9% (average: 5.2%) during extreme precipitation in Eastern Tianshan.

However, it also becomes clear from the results of the Lagrangian analysis that Central Asia, including the Tianshan itself, is the main moisture source of precipitation for the Tianshan in all seasons, especially for the Northern, Central, and Eastern Tianshan. Although moisture flux from East Asia and Siberia accounts for nearly 1/3 of the extreme precipitation in the Eastern Tianshan, the share of evaporation from local evaporation as well as from Central Asia remains the dominant source even in these extreme cases (64.7%). The increase of precipitation in the Tianshan seems to be closely related to evaporation in Central Asia and from local areas. Previous studies using the Eulerian approach have shown that the Atlantic Ocean, the Caspian Sea, and the Mediterranean Sea are important sources of precipitation in the Tianshan Mountains (Li et al., 2008; Ren et al., 2016; Guan et al., 2019). Jiang, Zhou, Wang, et al. (2020) also quantified the moisture source in Central Asia using the Eulerian source-tagging method with detailed atmospheric processes and concluded that the North Atlantic Ocean could explain up to 23% of the moisture source contribution to precipitation. However, according to the applied Lagrangian approach, the annual average moisture contributions of all oceanic sources to precipitation in the Western, Northern, Central, and Eastern Tianshan reaches only 9.1%, 8.1%, 5.4%, and 4.7%, respectively (Figure 8). Nevertheless, if the influence of the Northern Indian Ocean in winter is removed, then the Oceanic sources from the west including the Caspian Sea, the North Atlantic Ocean, and the Mediterranean Sea only account for 5.0%, 6.0%, 2.9%, and 3.8% of the Western, Northern, Central, and Eastern Tianshan, respectively. In accordance with results from S. Yao et al. (2021) our finding demonstrates that the contribution of these oceans, once considered an important source of moisture, is minimal on the climate scale. Taking the North Atlantic Ocean for example, it contributes not more than 5% to all Tianshan regions in all months according to the Lagrangian perspective. Only in November, it contributes nearly 5% moisture to the Northern and Eastern Tianshan guided

by a strong westerly component (Figure 8). These oceans certainly generate a significant amount of evaporation, which is transported by westerly winds to the Eurasian continent at mid-latitudes. However, a major part of the moisture from sea surfaces presumably is being lost to precipitation en route and possibly recycled several times by continental evaporation and precipitation before it eventually reaches the Tianshan via moisture uptake over Central Asia. Air masses in the desert areas of Central Asia are not supplemented by sufficient local moisture and continue to move eastward bringing precipitation to the western windward slopes of the Pamir Plateau and the Northern Tianshan but are unable to affect the Eastern and Central Tianshan (S. Wang et al., 2017). S. Wang et al. (2017) therefore pointed out that precipitation in the Tianshan is more likely to be evaporation of terrestrial moisture from Europe and Central Asia rather than direct oceanic moisture from the Atlantic Ocean. More attention should be paid to local evapotranspiration variations in predicting precipitation change in Xinjiang (Peng & Zhou, 2017). Zhou et al. (2019) also concluded that Xinjiang and Central Asia are key moisture sources for extreme precipitation in Xinjiang, with local contributions contributing 40% and 70% in the Ili Valley and Hami regions, respectively. These conclusions are consistent with our finding and also with the perspective that Xinjiang itself and Central Asia are the main sources of moisture contribution to precipitation in Xinjiang (S. Yao et al., 2021).

Central Asia has faced a significant temperature increase in recent decades, with rates of 0.36-0.42°C/10a for the period 1979-2011 and 0.34°C/10a for the period 1961-2016 in the Tianshan Mountains (Yuan-An et al., 2013; R. Hu, 2004). Rapid warming has led to a significant decrease in snow area and substantial glacier shrinkage in the Tianshan Mountains (Shangguan et al., 2015; J. Yao et al., 2022). The Central Asian regions with large glacier areas mainly show a trend of increasing runoff and increasing oasis area (Unger-Shayesteh et al., 2013; Y. Chen et al., 2016; X. Wang et al., 2020; J. Yao et al., 2022). In addition, a considerable and strong oasis expansion has occurred in Central Asia since the 1950s due to the rapid large-scale conversion of irrigation technology from traditional flood irrigation to modern drip irrigation systems (Q. Zhang et al., 2017). The oasis "irrigation effect" has a significant impact on increasing soil moisture, which in Central Asia tends to increase during 1950-2015, especially in northwest China (Z. Hu et al., 2019), leading to increased surface evaporation and atmospheric water vapor content (Kueppers & Snyder, 2012; M. Zhang et al., 2019). Surface cooling from enhanced evapotranspiration in turn modifies regional wind fields and enhances convective upward movement in the lower troposphere, providing

moisture and favorable dynamic conditions for enhanced local rainfall (J. Yao et al., 2020). All the above contributed to the increase of local moisture in the atmosphere, which also resulted in the increase of precipitation over Central Asia and the Tianshan Mountains (M. Zhang et al., 2019). However, it is worthwhile to note that although all are located in the same arid and semi-arid zone, areas in northwest China with glaciers experience a wetting trend, while northern China and Kazakhstan located in the centre of Central Asia without glaciers suffer from increasing aridity (J. Yao et al., 2022; Gerlitz et al., 2018; Z. Hu et al., 2017; Sorg et al., 2012). Peng and Zhou (2017) stated that the increasing trend of precipitation over northwest China is dominated by the thermodynamic component in association with changes in specific humidity, which is more important than the dynamic component due to changes in atmospheric circulation. Based on these facts, we hypothesize that the melting and retreat of the Tianshan glaciers and permafrost in recent decades may be contributing to increasing precipitation around the Tianshan and northwest China, as this mechanism, may locally to regionally provide additional moisture, leading to interdecadal change from "warm-dry" to "warm-wet" conditions. Thus, the rapid melting of glaciers caused by global warming may act as a driving factor to boost runoff and increase the area of oases, which leads to an increase in local water vapour from evaporation and eventually precipitation. This may act in terms of a positive feedback loop by increasing precipitation and in turn enhancing the oasis area and local evaporation (J. Yao et al., 2022). Under the long-term effect of this positive cycle, precipitation might increase in the Tianshan and Central Asia. However, the volume of mountain glacier ice is limited. Moreover, glacier retreat under progressing climate warming is irreversible on time scales of tens to hundreds of years. Thus, the "wetting" in Central Asia, including the Tianshan Mountains, is likely to be only a short-term fluctuation of the drying trend at the centennial-millennial scales (Jiang, Zhou, Chen, & Zhang, 2020; He et al., 2021). However, any quantitative analysis of the local water cycle including the contribution of meltwater from Tianshan glaciers lies beyond the scope and options of the current study.

Precipitation has not easily reproduced accurately in the Tianshan Mountains due to the scarcity of weather stations, especially at high altitudes. Although the correlation coefficient between precipitation in the Tianshan Mountains based on GPCC precipitation data and ERA-Interim data reaches 0.84 ($p \leq 0.01$), the temporal trends of precipitation still vary from region to region and even show opposite sign between GPCC and ERA-Interim data. In addition to the uncertainty of both the measured and spatially interpolated precipitation

data, and precipitation derived from numerical weather forecast reanalysis, the Lagrangian precipitation estimation in this study has its own limitations. As can be seen in (Figure 2), although the Lagrangian estimated precipitation captures the main characteristics of precipitation in the Tianshan Mountains, its value is larger than both the ERA-Interim and GPCC datasets. Such overestimation has previously been reported in studies using the Lagrangian method (Sodemann et al., 2008; Stohl & James, 2004; James et al., 2004; S. Yao et al., 2021). The main reason for the positive bias of estimated precipitation is due to the assumption that the decrease in Δq is completely counted as precipitation at the target location during the last 6 h before the starting point, rather than being allocated over the region that was traversed by the air mass during that final 6 h of the trajectory. Meanwhile, processes such as convection and the formation of ice crystals and water droplets during the cloud condensation process are neglected in the Lagrangian approach. In addition, as we mentioned in Section 3.1, all attributed moisture sources are considered as the sources of precipitation in Tianshan Mountains in this study. This follows the notion of Sodemann and Zubler (2010) who stated that if the distribution of moisture sources above and within the PBL performs similarly, then the moisture sources in the study area are not likely to differ significantly within and above the PBL. However, since only moisture uptake within the PBL can be directly linked to evaporation from the underlying surface, it is still possible that the absolute value and extent of moisture sources affecting precipitation in the Tianshan Mountains are overestimated to some degree.

5 Conclusion

In this study a Lagrangian method is used to identify the moisture source patterns of precipitation over the Tianshan Mountains and to analyse the quantitative contributions of the main moisture source areas during 1979-2017. All attributed moisture sources (evaporation within the PBL plus evaporation above the PBL) have been considered, with the highest evaporation contribution area mainly concentrated in Central Asia and locally in the Tianshan itself. The moisture source contributions vary both seasonally and between different sub-regions of the Tianshan Mountains. More long-range moisture transport exists during winter (November - March) due to the enhanced westerlies, especially for the Western Tianshan, while the moisture source distribution extends more northward and eastward in summer (April - October).

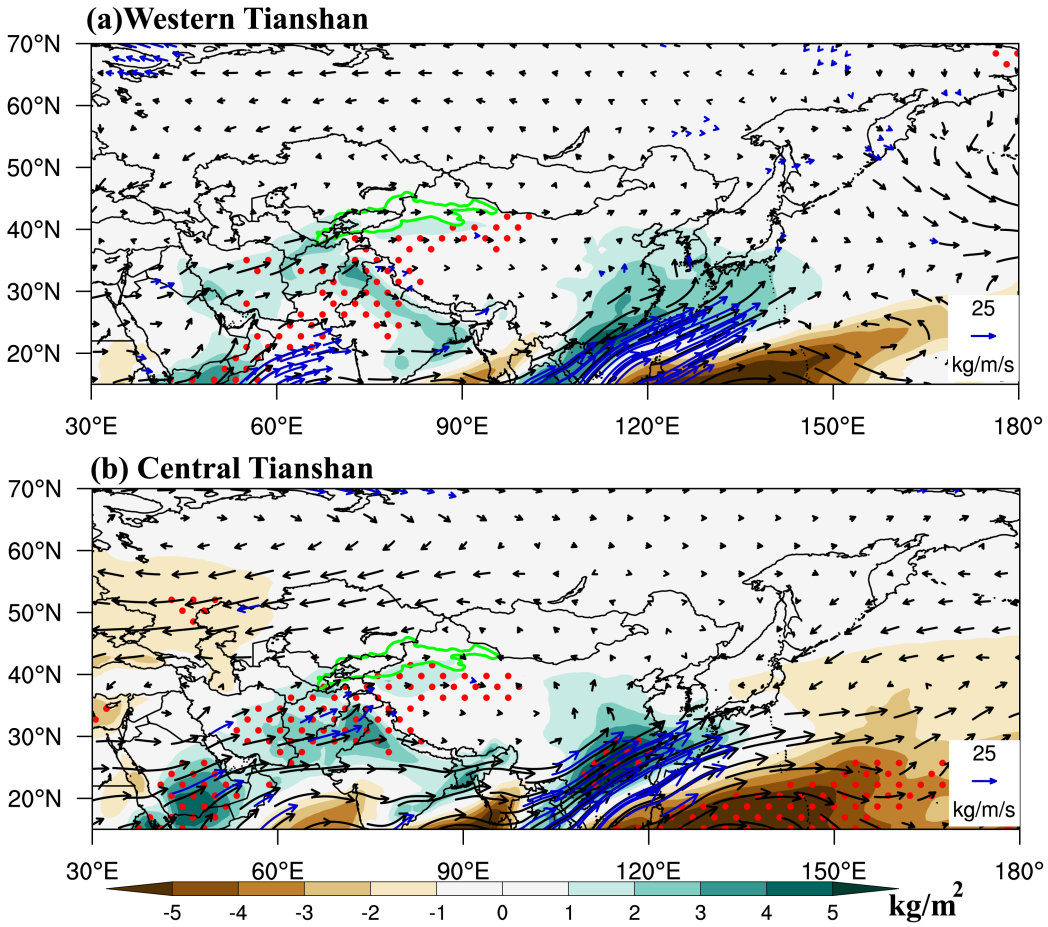

Figure 14. Anomalies of water vapour flux (vector in kg/m/s) and total precipitable water vapour content (PWC in kg/m^2) during extreme winter precipitation in (a) Western Tianshan; (b) Central Tianshan. Areas with red dots and the blue arrows indicate the anomalies of PWC and water vapour flux significant at the 95% confidence level, respectively.

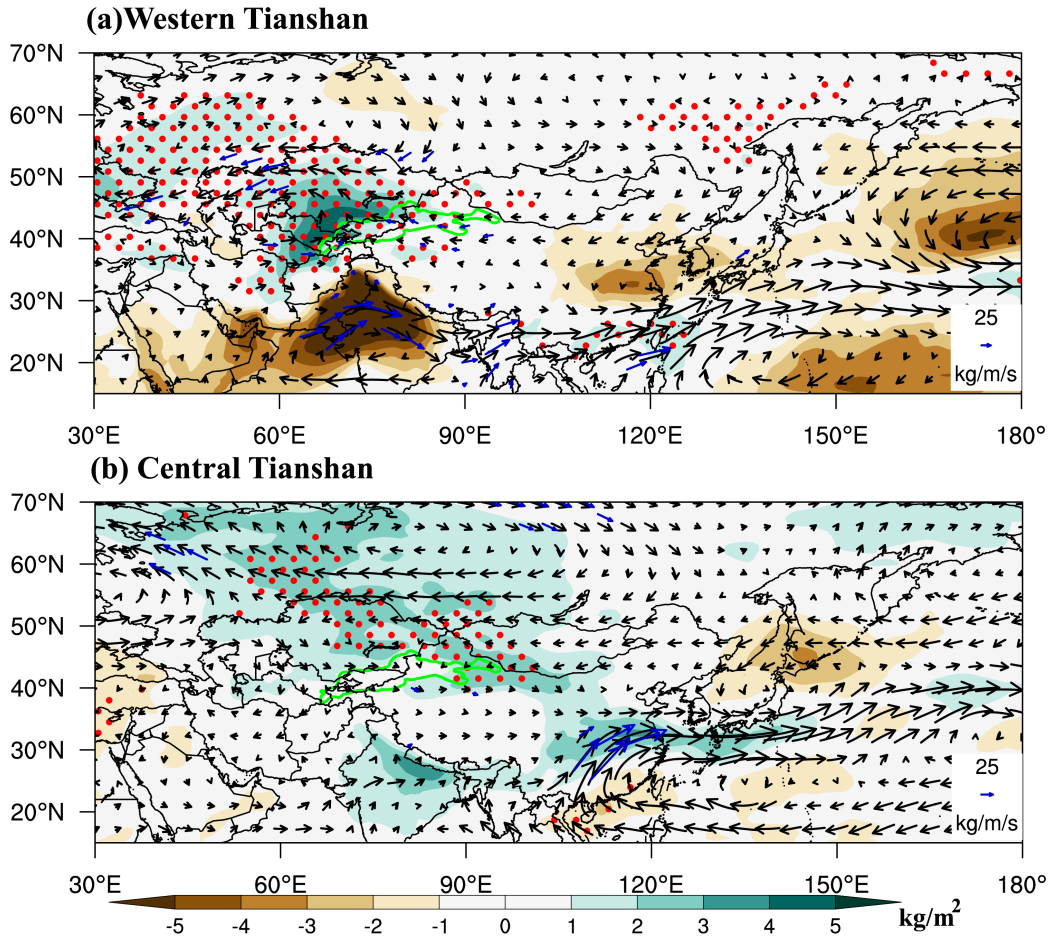

Figure 15. Anomalies of water vapour flux (vector in kg/m/s) and total precipitable water vapour content (PWC in kg/m^2) during extreme summer precipitation in (a) Western Tianshan; (b) Eastern Tianshan. Areas with red dots and the blue arrows indicate the anomalies of PWC and water vapour flux significant at the 95% confidence level, respectively.

Continental sources provide about 93.2% of the precipitation in the Tianshan. Specifically, continental sources contributed 90.9%, 91.9%, 94.6%, and 95.3% of the moisture to the Western, Northern, Central, and Eastern Tianshan, respectively. Among the continental sources, Central Asia plays a leading role in providing moisture for all sub-regions of the Tianshan Mountains. Excluding the indirect effect of moisture transport from the Ocean to nearby terrestrial land on precipitation in the Tianshan Mountains, the annual average moisture contribution directly from all Oceanic sources to precipitation in the Western, Northern, Central, and Eastern Tianshan reach 9.1%, 8.1%, 5.4%, and 4.7%, respectively.

For the Western Tianshan, the main contributors are Central Asia (31.8%) and West Asia (29.8%). These shares of these two moisture sources change between seasons. Moisture in summer months is advected mainly from Central Asia, with mean contributions of 41.0%, while in winter months it comes mainly from West Asia (45.7%). In addition, Tianshan itself supplies 17.2% of moisture contribution and the Indian Ocean provides 7.2% of the moisture to precipitation in winter for Western Tianshan. Central Asia and Tianshan itself explain 37.1% and 22.5% of the moisture contribution, respectively, and are identified as the main moisture source in the Northern Tianshan. Slightly further remote areas of West Asia and continental Europe also account for 19.5% and 7.3% of the contribution. For the precipitation of Central and Eastern Tianshan, we also identify local evaporation and Central Asia as the dominant moisture source, providing 66.8% and 69.9% of the moisture, respectively. It is followed by West Asia, which supplies 18.0% and 10.4% of moisture, respectively. In addition, 7.7% and 5.2% of moisture for precipitation in Eastern Tianshan originate from East and South Asia and Siberia in summer, which is different from all other Tianshan sub-regions.

From 1979-2017, there is no significant annual variation in the contribution of most moisture sources, including the predominant moisture source, Central Asia, for Western, Northern, and Central Tianshan. However, the contribution of moisture originating from Europe to precipitation for Central Tianshan and Eastern Tianshan all show a significant decreasing trend in summer with linear trends of -0.06mm/10a and -0.03mm/10a, respectively. The contribution of the North Atlantic Ocean to precipitation for Northern, Central, and Eastern Tianshan in summer also shows a decreasing trend with linear trends of -0.05mm/10a, -0.02mm/10a, and -0.01mm/10a, respectively, though it relative direct contribution to the Tianshan Mountains is limited anyway.

During extreme winter precipitation months, the largest increase of moisture in the Western Tianshan derives from West Asia (contribution in 54.1%). Apart from the evaporation from local and Central Asia, the gain of moisture from East and South Asia as well as Siberia in the Eastern Tianshan is obvious. Europe is also an important contributor to extreme precipitation months in the Northern Tianshan while for the Central Tianshan, on the other hand, the increase in local evaporation has the greatest impact on its extreme winter precipitation. Extreme summer precipitation months in the Tianshan Mountains are mainly caused by enhanced local evaporation and enhanced moisture flux from Central Asia. The Eastern Tianshan differs from other Tianshan regions in that moisture contribution from East and South Asia as well as Siberia increases significantly during periods with extreme precipitation.

Acknowledgments

We would like to thank the China Scholarship Council (CSC) for their support to Xuefeng Guan who is pursuing her Ph.D. degree at the Humboldt-Universität zu Berlin. We are also grateful to Tobias Sauter (Geography Department, Humboldt-Universität zu Berlin) and Junqiang Yao (Institute of Desert Meteorology, China Meteorological Administration) for valuable and fruitful discussions on earlier versions of the manuscript. We acknowledge support by the Open Access Publication Fund of the Humboldt-Universität zu Berlin.

Data Availability Statement: The ERA-Interim reanalysis data can be retrieved from the European Center from Medium-Range Weather Forecasts (`https://www.ecmwf.int/en/forecasts/datasets/reanalysis-datasets/era-interim`). The GPCC precipitation Data can be downloaded from Global Precipitation Climatology Centre (`https://www.dwd.de/EN/ourservices/gpcc/gpcc.html`).

We are pleased to make available to researchers interested in the monthly moisture sources of the Tianshan Mountains (1979-2017) obtained from the Lagrangian diagnostics. Xuefeng Guan, Lukas Langhamer, & Christoph Schneider. (2022). Moisture sources data of Tianshan Mountains [Data set]. Zenodo. https://doi.org/10.5281/zenodo.6320458

References

Aizen, V. B., Aizen, E. M., & Melack, J. M. (1995). Climate, snow cover, glaciers, and runoff

in the tien shan, central asia 1. *JAWRA Journal of the American Water Resources Association*, *31*(6), 1113–1129.

Aizen, V. B., Aizen, E. M., Melack, J. M., & Dozier, J. (1997). Climatic and hydrologic changes in the tien shan, central asia. *Journal of Climate*, *10*(6), 1393–1404.

Aizen, V. B., Kuzmichenok, V. A., Surazakov, A. B., & Aizen, E. M. (2006). Glacier changes in the central and northern tien shan during the last 140 years based on surface and remote-sensing data. *Annals of Glaciology*, *43*, 202–213.

Armstrong, R. L., Rittger, K., Brodzik, M. J., Racoviteanu, A., Barrett, A. P., Khalsa, S.-J. S., ... others (2019). Runoff from glacier ice and seasonal snow in high asia: separating melt water sources in river flow. *Regional Environmental Change*, *19*(5), 1249–1261.

Bekturganov, Z., Tussupova, K., Berndtsson, R., Sharapatova, N., Aryngazin, K., & Zhanasova, M. (2016). Water related health problems in central asia—a review. *Water*, *8*(6), 219.

Berrisford, P., Kållberg, P., Kobayashi, S., Dee, D., Uppala, S., Simmons, A., ... Sato, H. (2011). Atmospheric conservation properties in era-interim. *Quarterly Journal of the Royal Meteorological Society*, *137*(659), 1381–1399.

Bothe, O., Fraedrich, K., & Zhu, X. (2012). Precipitation climate of central asia and the large-scale atmospheric circulation. *Theoretical and applied climatology*, *108*(3), 345–354.

Boutle, I. A., Belcher, S. E., & Plant, R. S. (2011). Moisture transport in midlatitude cyclones: Cyclone moisture transport. , *137*(655), 360–373. Retrieved 2022-02-15, from `https://onlinelibrary.wiley.com/doi/10.1002/qj.783` doi: 10.1002/qj.783

Chen, S., Gan, T. Y., Tan, X., Shao, D., & Zhu, J. (2019). Assessment of cfsr, era-interim, jra-55, merra-2, ncep-2 reanalysis data for drought analysis over china. *Climate Dynamics*, *53*(1), 737–757.

Chen, Y., Li, W., Deng, H., Fang, G., & Li, Z. (2016). Changes in central asia's water tower: past, present and future. *Scientific reports*, *6*(1), 1–12.

Dee, D. P., Uppala, S. M., Simmons, A. J., Berrisford, P., Poli, P., Kobayashi, S., ... others (2011). The era-interim reanalysis: Configuration and performance of the data assimilation system. *Quarterly Journal of the royal meteorological society*, *137*(656), 553–597.

Durán-Quesada, A. M., Gimeno, L., Amador, J., & Nieto, R. (2010). Moisture sources

for central america: Identification of moisture sources using a lagrangian analysis technique. *Journal of Geophysical Research: Atmospheres*, *115*(D5).

Fan, M., Xu, J., Li, D., & Chen, Y. (2022). Response of precipitation in tianshan to global climate change based on the berkeley earth and era5 reanalysis products. *Remote Sensing*, *14*(3), 519.

Farinotti, D., Longuevergne, L., Moholdt, G., Duethmann, D., Mölg, T., Bolch, T., ... Güntner, A. (2015). Substantial glacier mass loss in the tien shan over the past 50 years. *Nature Geoscience*, *8*(9), 716–722.

Feng, F., Li, Z., Zhang, M., Jin, S., & Dong, Z. (2013). Deuterium and oxygen 18 in precipitation and atmospheric moisture in the upper urumqi river basin, eastern tianshan mountains. *Environmental Earth Sciences*, *68*(4), 1199–1209.

Freedman, D., Pisani, R., & Purves, R. (2007). Statistics (international student edition). *Pisani, R. Purves, 4th edn. WW Norton & Company, New York*.

Gao, Y., Xiao, L., Chen, D., Xu, J., & Zhang, H. (2018). Comparison between past and future extreme precipitations simulated by global and regional climate models over the tibetan plateau. *International Journal of Climatology*, *38*(3), 1285–1297.

Gerlitz, L., Conrad, O., Thomas, A., & Böhner, J. (2014). Warming patterns over the tibetan plateau and adjacent lowlands derived from elevation-and bias-corrected era-interim data. *Climate research*, *58*(3), 235–246.

Gerlitz, L., Steirou, E., Schneider, C., Moron, V., Vorogushyn, S., & Merz, B. (2018). Variability of the cold season climate in central asia. part i: weather types and their tropical and extratropical drivers. *Journal of climate*, *31*(18), 7185–7207.

Gimeno, L., Nieto, R., Trigo, R. M., Vicente-Serrano, S. M., & López-Moreno, J. I. (2010). Where does the iberian peninsula moisture come from? an answer based on a lagrangian approach. *Journal of Hydrometeorology*, *11*(2), 421–436.

Gimeno, L., Stohl, A., Trigo, R. M., Dominguez, F., Yoshimura, K., Yu, L., ... Nieto, R. (2012). Oceanic and terrestrial sources of continental precipitation. *Reviews of Geophysics*, *50*(4).

Guan, X., Yang, L., Zhang, Y., & Li, J. (2019). Spatial distribution, temporal variation, and transport characteristics of atmospheric water vapor over central asia and the arid region of china. *Global and Planetary Change*, *172*, 159–178.

Guan, X., Yao, J., & Schneider, C. (2021a). Variability of the precipitation over the tianshan mountains, central asia. part ii: Multi-decadal precipitation trends and their

association with atmospheric circulation in both the winter and summer seasons. *International Journal of Climatology*.

Guan, X., Yao, J., & Schneider, C. (2021b). Variability of the precipitation over the tianshan mountains, central asia. part i: Linear and nonlinear trends of the annual and seasonal precipitation. *International Journal of Climatology*.

Guo, Y., Xu, X., Chen, W., Wei, F., & Chen, A. (2014). Heat source over 'fishtail'type topography effects on tianshan mountain regions precipitation systems and water resources. *Plateau Meteorology*, *33*(5), 1363–1373.

Hamm, A., Arndt, A., Kolbe, C., Wang, X., Thies, B., Boyko, O., ... Schneider, C. (2020). Intercomparison of gridded precipitation datasets over a sub-region of the central himalaya and the southwestern tibetan plateau. *Water*, *12*(11), 3271.

He, H., Luo, G., Cai, P., Hamdi, R., Termonia, P., De Maeyer, P., ... Li, J. (2021). Assessment of climate change in central asia from 1980 to 2100 using the köppen-geiger climate classification. *Atmosphere*, *12*(1), 123.

Hu, R. (2004). Physical geography of the tianshan mountains in china. *China Environmental Science Press, Beijing*, 264–273.

Hu, Z., Chen, X., Chen, D., Li, J., Wang, S., Zhou, Q., ... Guo, M. (2019). "dry gets drier, wet gets wetter": A case study over the arid regions of central asia. *International Journal of Climatology*, *39*(2), 1072–1091.

Hu, Z., Hu, Q., Zhang, C., Chen, X., & Li, Q. (2016). Evaluation of reanalysis, spatially interpolated and satellite remotely sensed precipitation data sets in central asia. *Journal of Geophysical Research: Atmospheres*, *121*(10), 5648–5663.

Hu, Z., Zhang, C., Hu, Q., & Tian, H. (2014). Temperature changes in central asia from 1979 to 2011 based on multiple datasets. *Journal of Climate*, *27*(3), 1143–1167.

Hu, Z., Zhou, Q., Chen, X., Qian, C., Wang, S., & Li, J. (2017). Variations and changes of annual precipitation in central asia over the last century. *International Journal of Climatology*, *37*, 157–170.

Hua, L., Zhong, L., & Ma, Z. (2017). Decadal transition of moisture sources and transport in northwestern china during summer from 1982 to 2010. *Journal of Geophysical Research: Atmospheres*, *122*(23), 12–522.

Huang, W., Chang, S.-Q., Xie, C.-L., & Zhang, Z.-P. (2017). Moisture sources of extreme summer precipitation events in north xinjiang and their relationship with atmospheric circulation. *Advances in Climate Change Research*, *8*(1), 12–17.

Huang, W., Chen, F., Feng, S., Chen, J., & Zhang, X. (2013). Interannual precipitation variations in the mid-latitude asia and their association with large-scale atmospheric circulation. *Chinese Science Bulletin*, *58*(32), 3962–3968.

Huang, W., Chen, J., Zhang, X., Feng, S., & Chen, F. (2015). Definition of the core zone of the "westerlies-dominated climatic regime", and its controlling factors during the instrumental period. *Science China Earth Sciences*, *58*(5), 676–684.

Immerzeel, W., & Bierkens, M. (2012). Asia's water balance. *Nature Geoscience*, *5*(12), 841–842.

James, P., Stohl, A., Spichtinger, N., Eckhardt, S., & Forster, C. (2004). Climatological aspects of the extreme european rainfall of august 2002 and a trajectory method for estimating the associated evaporative source regions. *Natural Hazards and Earth System Sciences*, *4*(5/6), 733–746.

Jiang, J., Zhou, T., Chen, X., & Zhang, L. (2020). Future changes in precipitation over central asia based on cmip6 projections. *Environmental Research Letters*, *15*(5), 054009.

Jiang, J., Zhou, T., Wang, H., Qian, Y., Noone, D., & Man, W. (2020). Tracking moisture sources of precipitation over central asia: A study based on the water-source-tagging method. *Journal of Climate*, *33*(23), 10339–10355.

Kendall, M. (1975). *Rank correlation measures (london: Charles griffin).*

Knippertz, P., & Wernli, H. (2010). A lagrangian climatology of tropical moisture exports to the northern hemispheric extratropics. *Journal of Climate*, *23*(4), 987–1003.

Kueppers, L. M., & Snyder, M. A. (2012). Influence of irrigated agriculture on diurnal surface energy and water fluxes, surface climate, and atmospheric circulation in california. *Climate Dynamics*, *38*(5), 1017–1029.

Langhamer, L., Dublyansky, Y., & Schneider, C. (2021). Spatial and temporal planetary boundary layer moisture-source variability of crimean peninsula precipitation. *Earth and Space Science*, e2021EA001727.

Langhamer, L., Sauter, T., & Mayr, G. J. (2018). Lagrangian detection of moisture sources for the southern patagonia icefield (1979–2017). *Frontiers in Earth Science*, 219.

Lemenkova, P. (2013). Current problems of water supply and usage in central asia, tian shan basin. In *Environmental and climate technologies. proceedings of 54th international scientific conference (riga technical university, institute of energy systems and environment).*

Li, W., Wang, K., Fu, S., & Jiang, H. (2008). The interrelationship between regional

westerly index and the water vapor budget in northwest china. *Journal of Glaciology and Geocryology*, *30*(1), 28–34.

Liu, J., Liu, F., Tuoliewubieke, D., & Yang, L. (2020). Analysis of the water vapour transport and accumulation mechanism during the "7.31" extreme rainstorm event in the southeastern hami area, china. *Meteorological Applications*, *27*(4), e1933.

Liu, J., & Zhang, W. (2017). Long term spatio-temporal analyses of snow cover in central asia using era-interim and modis products. In *Iop conference series: Earth and environmental science* (Vol. 57, p. 012033).

Mann, H. (1945). *Non-parametric tests against trend. econometria.* Chicago.

Mariotti, A. (2007). How enso impacts precipitation in southwest central asia. *Geophysical research letters*, *34*(16).

Nieto, R., Gimeno, L., & Trigo, R. M. (2006). A lagrangian identification of major sources of sahel moisture. *Geophysical Research Letters*, *33*(18).

Oh, H., Jhun, J.-G., Ha, K.-J., & Seo, K.-H. (2017). Combined effect of the east atlantic/west russia and western pacific teleconnections on the east asian winter monsoon. *Asia-Pacific Journal of Atmospheric Sciences*, *53*(2), 273–285.

Ososkova, T., Gorelkin, N., & Chub, V. (2000). Water resources of central asia and adaptation measures for climate change. *Environmental monitoring and assessment*, *61*(1), 161–166.

Owens, R., & Hewson, T. (2018). Ecmwf forecast user guide. *Reading: ECMWF*, *10*, m1cs7h.

Peng, D., & Zhou, T. (2017). Why was the arid and semiarid northwest china getting wetter in the recent decades? *Journal of Geophysical Research: Atmospheres*, *122*(17), 9060–9075.

Pfahl, S., Madonna, E., Boettcher, M., Joos, H., & Wernli, H. (2014). Warm conveyor belts in the ERA-interim dataset (1979–2010). part II: Moisture origin and relevance for precipitation. , *27*(1), 27–40. Retrieved 2022-02-15, from `http://journals.ametsoc.org/doi/10.1175/JCLI-D-13-00223.1` doi: 10.1175/JCLI-D-13-00223.1

Ramos, A. M., Nieto, R., Tomé, R., Gimeno, L., Trigo, R. M., Liberato, M. L., & Lavers, D. A. (2016). Atmospheric rivers moisture sources from a lagrangian perspective. *Earth System Dynamics*, *7*(2), 371–384.

Ren, G., Yuan, Y., Liu, Y., Ren, Y., Wang, T., & Ren, X. (2016). Changes in precipitation over northwest china. *Arid zone research*, *33*(1), 1–19.

Schiemann, R., Lüthi, D., Vidale, P. L., & Schär, C. (2008). The precipitation climate of central asia—intercomparison of observational and numerical data sources in a remote semiarid region. *International Journal of Climatology: A Journal of the Royal Meteorological Society*, *28*(3), 295–314.

Schneider, U., Becker, A., Finger, P., Meyer-Christoffer, A., & Ziese, M. (2018). Gpcc full data monthly product version 2018 at 0.25°: Monthly land-surface precipitation from rain-gauges built on gts-based and historical data. *GPCC: Offenbach, Germany*.

Schuster, L., Maussion, F., Langhamer, L., & Moseley, G. E. (2021). Lagrangian detection of precipitation moisture sources for an arid region in northeast greenland: relations to the north atlantic oscillation, sea ice cover, and temporal trends from 1979 to 2017. *Weather and Climate Dynamics*, *2*(1), 1–17.

Shangguan, D. H., Bolch, T., Ding, Y., Kröhnert, M., Pieczonka, T., Wetzel, H.-U., & Liu, S. (2015). Mass changes of southern and northern inylchek glacier, central tian shan, kyrgyzstan, during 1975 and 2007 derived from remote sensing data. *The Cryosphere*, *9*(2), 703–717.

Sodemann, H., Schwierz, C., & Wernli, H. (2008). Interannual variability of greenland winter precipitation sources: Lagrangian moisture diagnostic and north atlantic oscillation influence. *Journal of Geophysical Research: Atmospheres*, *113*(D3).

Sodemann, H., & Zubler, E. (2010). Seasonal and inter-annual variability of the moisture sources for alpine precipitation during 1995–2002. *International Journal of Climatology: A Journal of the Royal Meteorological Society*, *30*(7), 947–961.

Song, M.-y., Li, Z.-q., Xia, D.-s., Jin, S., & Zhang, X. (2019). Isotopic evidence for the moisture origin and influencing factors at urumqi glacier no. 1 in upstream urumqi river basin, eastern tianshan mountains. *Journal of Mountain Science*, *16*(8), 1802–1815.

Sorg, A., Bolch, T., Stoffel, M., Solomina, O., & Beniston, M. (2012). Climate change impacts on glaciers and runoff in tien shan (central asia). *Nature Climate Change*, *2*(10), 725–731.

Sprenger, M., & Wernli, H. (2015). The lagranto lagrangian analysis tool–version 2.0. *Geoscientific Model Development*, *8*(8), 2569–2586.

Stohl, A., & James, P. (2004). A lagrangian analysis of the atmospheric branch of the global water cycle. part i: Method description, validation, and demonstration for the august 2002 flooding in central europe. *Journal of Hydrometeorology*, *5*(4), 656–678.

Sun, B., & Wang, H. (2014). Moisture sources of semiarid grassland in china using the lagrangian particle model flexpart. *Journal of Climate*, *27*(6), 2457–2474.

Unger-Shayesteh, K., Vorogushyn, S., Farinotti, D., Gafurov, A., Duethmann, D., Mandychev, A., & Merz, B. (2013). What do we know about past changes in the water cycle of central asian headwaters? a review. *Global and Planetary Change*, *110*, 4–25.

Wang, S., Zhang, M., Crawford, J., Hughes, C. E., Du, M., & Liu, X. (2017). The effect of moisture source and synoptic conditions on precipitation isotopes in arid central asia. *Journal of Geophysical Research: Atmospheres*, *122*(5), 2667–2682.

Wang, S., Zhang, M., Sun, M., Wang, B., & Li, X. (2013). Changes in precipitation extremes in alpine areas of the chinese tianshan mountains, central asia, 1961–2011. *Quaternary International*, *311*, 97–107.

Wang, W., Li, H., Wang, J., & Hao, X. (2020). Water vapor from western eurasia promotes precipitation during the snow season in northern xinjiang, a typical arid region in central asia. *Water*, *12*(1), 141.

Wang, X., Yang, T., Xu, C.-Y., Xiong, L., Shi, P., & Li, Z. (2020). The response of runoff components and glacier mass balance to climate change for a glaciated high-mountainous catchment in the tianshan mountains. *Natural Hazards*, *104*(2), 1239–1258.

Weigel, A. P., Chow, F. K., & Rotach, M. W. (2007). The effect of mountainous topography on moisture exchange between the "surface" and the free atmosphere. *Boundary-Layer Meteorology*, *125*(2), 227–244.

Wernli, H., & Davies, H. C. (1997). A lagrangian-based analysis of extratropical cyclones. i: The method and some applications. *Quarterly Journal of the Royal Meteorological Society*, *123*(538), 467–489.

Winschall, A., Pfahl, S., Sodemann, H., & Wernli, H. (2014). Comparison of eulerian and lagrangian moisture source diagnostics–the flood event in eastern europe in may 2010. *Atmospheric Chemistry and Physics*, *14*(13), 6605–6619.

Xenarios, S., Gafurov, A., Schmidt-Vogt, D., Sehring, J., Manandhar, S., Hergarten, C., ... Foggin, M. (2019). Climate change and adaptation of mountain societies in central asia: uncertainties, knowledge gaps, and data constraints. *Regional Environmental Change*, *19*(5), 1339–1352.

Xingang, D., Weijing, L., Zhuguo, M., & Ping, W. (2007). Water-vapor source shift of xinjiang region during the recent twenty years. *Progress in natural science*, *17*(5),

569–575.

Yang, Q., & He, Q. (2003). Climate change in the western tianshan mountainous and climate effect of oasis. *Journal of Glaciology and Geocryology*, *3*.

Yao, J., Chen, Y., Guan, X., Zhao, Y., Chen, J., & Mao, W. (2022). Recent climate and hydrological changes in a mountain–basin system in xinjiang, china. *Earth-Science Reviews*, 103957.

Yao, J., Chen, Y., Zhao, Y., Guan, X., Mao, W., & Yang, L. (2020). Climatic and associated atmospheric water cycle changes over the xinjiang, china. *Journal of Hydrology*, *585*, 124823.

Yao, J., Liu, X., & Hu, W. (2021). Stable isotope compositions of precipitation over central asia. *PeerJ*, *9*, e11312.

Yao, S., Jiang, D., & Zhang, Z. (2021). Lagrangian simulations of moisture sources for chinese xinjiang precipitation during 1979–2018. *International Journal of Climatology*, *41*, E216–E232.

Yatagai, A., Kamiguchi, K., Arakawa, O., Hamada, A., Yasutomi, N., & Kitoh, A. (2012). Aphrodite: Constructing a long-term daily gridded precipitation dataset for asia based on a dense network of rain gauges. *Bulletin of the American Meteorological Society*, *93*(9), 1401–1415.

Yuan, Y., He, Q., & Yu, S. (2004). Feature of annual precipitation change in tianshan mountain area for the recent 40 years and comparison with those in the south and north xinjiang. *Scientia Meteorological Sinica*, *24*, 220–226.

Yuan-An, J., Ying, C., Yi-Zhou, Z., Peng-Xiang, C., Xing-Jie, Y., Jing, F., & Su-Qin, B. (2013). Analysis on changes of basic climatic elements and extreme events in xinjiang, china during 1961–2010. *Advances in Climate Change Research*, *4*(1), 20–29.

Zeng, X., Brunke, M. A., Zhou, M., Fairall, C., Bond, N. A., & Lenschow, D. H. (2004). Marine atmospheric boundary layer height over the eastern pacific: Data analysis and model evaluation. *Journal of Climate*, *17*(21), 4159–4170.

Zhang, H., Ouyang, Z., Zheng, H., & Wang, X. (2009). Recent climate trends on the northern slopes of the tianshan mountains, xinjiang, china. *Journal of Mountain Science*, *6*(3), 255–265.

Zhang, M., Luo, G., Cao, X., Hamdi, R., Li, T., Cai, P., ... He, H. (2019). Numerical simulation of the irrigation effects on surface fluxes and local climate in typical mountain-oasis-desert systems in the central asia arid area. *Journal of Geophysical*

Research: Atmospheres, *124*(23), 12485–12506.

Zhang, Q., Luo, G., Li, L., Zhang, M., Lv, N., & Wang, X. (2017). An analysis of oasis evolution based on land use and land cover change: A case study in the sangong river basin on the northern slope of the tianshan mountains. *Journal of Geographical Sciences*, *27*(2), 223–239.

Zhao, P., Gao, L., Wei, J., Ma, M., Deng, H., Gao, J., & Chen, X. (2020). Evaluation of era-interim air temperature data over the qilian mountains of china. *Advances in Meteorology*, *2020*.

Zhou, Y.-s., Xie, Z.-m., & Liu, X. (2019). An analysis of moisture sources of torrential rainfall events over xinjiang, china. *Journal of Hydrometeorology*, *20*(10), 2109–2122.